ADVANCED MATERIALS INTERFACES
www.advmatinterfaces.de

Recent Development of Liquid Metal-Based Functional Materials Combined with Common Transition Metals

Yang Wang, Jiarui Guo, Wenlong Xiao, Kang Sun, Hongzhang Wang, and Liang Hu**

Gallium-based liquid metals (LMs) are a group of metal materials that are in liquid state at room temperature. Their unique physiochemical properties such as fluidity, conductivity, and interfacial properties with other materials have presented great potentials and wide applications. Specifically, the interactions between gallium-based LMs and some common but important transition metals (TMs) have not only enabled a series of intriguing phenomena but also provided valuable strategies or functional materials in soft robotics, devices, flexible electronics, addictive manufacturing, biomedical engineering and therapies, and other fields. The chemical mechanisms including the galvanic corrosion, infiltration, intermetallic compound formation should play vital roles within these interactions. Hereby the combining the LMs and TMs by alloying or physically mixing may offer a platform to develop novel and multifunctional materials system. To acquire a comprehensive understanding of those interactions as well as to inspire the researches for multifunctional materials design and applications, this article reviews the researches on the combination of LMs and TMs, discusses the characteristics, the mechanisms, and their applications especially in electronics, smart materials, and biomedicine. The main challenges and future research outlook are also discussed.

1. Introduction

Gallium-based eutectic alloys, represented by EGaIn (Ga 75, In 25 wt%) and Galinstan (Ga 68.5, In 21.5, Sn 10, wt%), are a group of metals that are in liquid state at room temperature.[1–3] They not only share the common properties of metals such as high thermal[1] and electrical conductivity,[3] but also own intriguing properties such as fluidity, transformability, and low viscosity.[2] Thus they demonstrate superiority as flexible conductors or electrical components. Generally they have low melting points (EGaIn: 15.9 °C, Galinstan: –19 °C) and high surface tension (624 mN m^{-1}).[2] More specifically, a thin oxide layer can easily form over the liquid metals (LMs) in an aerobic environment (including solutions with dissolved oxygen such as water, ethanol, etc.).[4] This oxide layer can be resembled to the skin of LMs, with a thickness of about 1–3 nm,[3,5] protecting the internal LMs from being further oxidized. Simultaneously, the oxide film can be used as a surfactant, greatly reducing the surface tension of the LMs.[6] Distinctively, the oxide layer can be generated and removed by applying voltage or adjusting the pH value of the solution environment.[7–10] This feature makes it possible to control the deformation and motivation of LMs, which is also an important principle of LM-based actuator design. Owing to these special physics and chemistry properties, LMs have abundant applications in thermal management,[11–13] 3D printing,[14–17] flexible electronics,[1,14,18–22] catalysts,[23–26] cancer treatment,[27–29] and other fields. In the aspect of flexible electronic materials, LMs have inherent advantages over the widely used solid metallic conductors such as copper, iron, gold, silver, and platinum. However, the high surface tension of LMs usually has negative effects on the patterning as well as the resolution.[15,16,30,31] What's more, the low viscosity affects the adhesion between LMs and other interfaces and increases the fluidity, which is not conducive to the processing of LM electronic circuits, such as printing on planar substrate.[17,32–34] Recently studies have proposed to change the surface tension and viscosity of LMs by metal doping or combining with other metals, mostly transition metals (TMs).[33,35–37] Moreover, the combination of LMs and some metals by physically mixing or chemically alloying can achieve multifunctional materials such as intelligent drivable, enhanced electrical conductive, or magnetic materials.[18,38] For example, addition of magnetic metals into LMs endows the composites with ability of magnetic control. This series of research shows the potential application in the release of drugs, rehabilitation equipment, and functional flexible electronics.[39–42] Some biologically

Y. Wang, K. Sun, L. Hu
Beijing Advanced Innovation Center for Biomedical Engineering
Beihang University
Beijing 100191, China
E-mail: cnhuliang@buaa.edu.cn
J. Guo
Beijing Research Institute of Mechanical Equipment
Beijing 100191, China
W. Xiao
Key Laboratory of Aerospace Advanced Materials and Performance of Ministry of Education
School of Materials Science and Engineering
Beihang University
Beijing 100191, China
H. Wang
Department of Biomedical Engineering
School of Medicine
Tsinghua University
Beijing 100084, China
E-mail: wanghz15@tsinghua.org.cn

The ORCID identification number(s) for the author(s) of this article can be found under https://doi.org/10.1002/admi.202100884.

DOI: 10.1002/admi.202100884

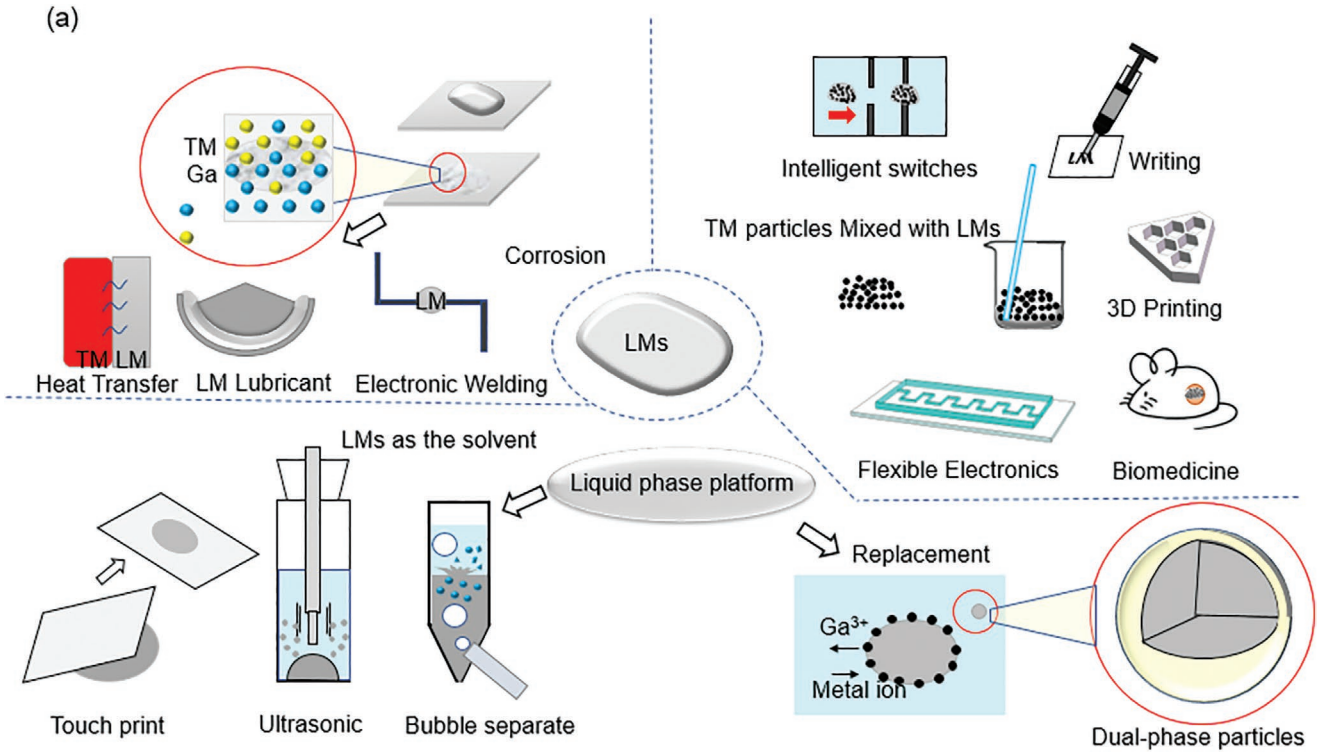

Figure 1. The combination and application between LMs and TMs. The first section (top left) describes the corrosion between TMs and LMs, which can be applied in heat transfer, lubricant, and electronic weilding materials. The second section (top right) introduces the composite materials containing LMs and TM particles, which can be applied in flexible electronics, biomedicine, and 3D printing inks. The third section (bottom) suggests the LM can bear the function of a liquid platform. On the one hand, the liquid phase structure which had dissolved other metals was destroyed by ultrasonic, bubble, or adhesion to prepare nanometals; on the other hand, reducibility of LM can be used to replace TM and form biphase metal materials.

unfriendly transition metals such as copper could be modified by forming alloy with LMs to improve their biocompatibility and reduce the toxicity.[14,43]

From this perspective, combination between the LMs and other metals by alloying or physically mixing offers a method to develop the novel and multifunctional materials. In this review, we focus on the combination of LMs with most common but important TMs such as copper, iron, gold, silver, and platinum. These TMs have a long history of development in human civilization with abundant reserves. In general, these TMs are chemically stable and environmentally safe in the ambient environment. Thus they have been widely used in machine manufacturing,[44] transportation,[45] electronic devices,[46] aerospace,[47] material design.[48] Owing to the excellent features of LMs, the combination of TMs and LMs creates more possibilities for modern technology. It is found that the combination of LMs and TMs can be classified into three conditions: corrosion between LMs and TMs substrate, mixing of LMs and TM Particles, and preparation of new TM materials using LMs as a liquid platform shown in **Figure 1**. The corrosion often occurs when LMs are used for heat dissipation, electronic welding,[20,42] liquid lubricant and some applications at high temperature conditions. Therefore, it is necessary to study the corrosion mechanism, process, and protection methods. At the same time, the multifunctional composite materials prepared by the mixing of TMs powder and LMs, are widely used in printing,[14,15] flexible devices, intelligent switches, biomedical, and other fields. It is worth noting that using LMs as a liquid phase platform, TMs elements can be dissolved in LMs, and micro-nano TMs can be released and prepared by using ultrasound, pulse voltage, interface destruction, which is a new method with low cost and low energy consumption. The preparation of biphasic metal[24] particles with LMs has inspired scholars to conduct further research and exploration of on the combination of transition metals and LM.[49,50] In this review, we comprehensively summarize the combination of LMs and several common TMs including their physiochemical characteristics, combination mechanisms and applications.[51–53] The research prospect is also put forward at the end of this work.

2. The Characteristics of the Combination of LMs and TMs

Combining TMs with LMs will generate new features and functionalities that do not exist in either of them. For example, mixing LMs and TMs, such as Ni, Cu, and Ag fabricates a semiliquid material, which can be applied for highly conductive electronic welding. At the same time, the trade-off is that LMs will corrode some TMs and bring potential dangers. Therefore, exploring the reaction conditions and characteristics of LMs and TMs in different external environments can not only bring more application value, but also effectively prevent the occurrence of metal corrosion. **Table 1**[24,26,51–57] shows the conventional resultants of a combination of LMs and different

Table 1. Intermetallic compounds made of LMs and TMs.

Reactant	Resultant	Temperature	Reference
Fe	$FeGa_3$	200–824 °C	[58–60]
Cu	θ-$CuGa_2$	29.8–254 °C	[55,61]
	γ-$CuGa_2$	>254 °C	[62,63]
Pt	Pt_5Ga	Room temperature	[23]
	$GaPt_3$	280 °C	[64,65]
	Ga_2Pt	160 °C	[66]
Ag	Ag_2Ga	Room temperature	[67]
	Ag_3Ga	100 °C	[53]
Au	$AuGa_2$	29.8–491 °C	[68,69]

TMs under different reaction condition. The velocity and morphology of the composites can be controlled by regulating the reaction conditions, which creates the possibility for new applications of LMs and TMs. For the clearly presenting, we summarize the characteristics of the combination of LMs with TMs.

2.1. The Combination of LMs and Fe

2.1.1. Corrosion between LMs and Fe

LMs have excellent thermal conductivity and fluidity to be a potential heat conduction and heat dissipation medium in terms of thermal management.[11,12] Although LMs do not have high thermal conductivity comparing with liquid Na and Li,[32] their chemical properties are more stable[18,70] and they are difficult to combustion and explosion at high temperature. Therefore LMs are more suitable for heat dissipation in nuclear engineering and other high temperature environment.[13,71] But LMs tend to corrode with stainless steel,[49,50] iron, copper,[51,55] aluminum,[10,72] and other metals.

Researches on the combination of LMs and ferrous materials, especially corrosion-related phenomena, are important in thermal management. LMs can corrode stainless steel, which was originally reported by Barbiera et al. in 1997.[49] They found that martensite and austenite were severely corroded by LMs at 400 °C, with the main product $FeGa_3$. **Figure 2**a shows the cross-sectional morphology photos of 1.4914 martensitic steel and 316 L austenitic steel after corrosion in liquid gallium for 307 h. The growth kinetics of the generated alloy compounds reaction layer was affected by the mutual dissolution rate, material composition, and structure, etc., thus different growth morphology layer was formed. In Cui et al.'s study,[28] LMs could corrode 304 stainless steel at 200 and 400 °C. With the temperature getting higher, the corrosion would be more severe. It was noteworthy that at 100 °C, there was nearly no trace of corrosion. Figure 2b shows the photo of the LMs corroding iron plate at 200 °C for 2 h. The corrosion trace could be observed clearly after removing the LMs. Energy dispersive spectrometer (EDS) shown in Figure 2c indicates that gallium molar concentration in the corrosive area was about 4.12%, oxygen molar concentration was about 43.41%, and indium was not detected. Corrosion only occurred on the surface and EGaIn did not penetrate the interior. The main formations were iron-based compound and chromium-based compound. In the X-ray diffraction (XRD) analysis, $FeGa_3$ and Cr_3Ga_4 were found. Figure 2d is optical photographs of the edge of the stainless steel sample corroded by at 500 °C for 17 and 700 h.[50] For longer reaction time, the degree of corrosion increased dramatically and the weight of the steel was significantly reduced after corrosion. From the researches of corrosion between LMs and stainless steel, it can be concluded that LMs and Fe-based materials will corrode without special protection. As the temperature rises, the corrosion will become more and more serious. LMs directly used as heat sink for Fe-based materials are not so suitable, because long-term corrosion will bring safety hazards to the system.

Corrosion between LMs and austenite, martensite, and other steel materials severely limits LMs as heat dissipation fluid applications and industrial thermal management. Adding a protective layer such as SiO_2 can help prevent corrosion, but how to effectively prevent the corrosion of LMs and steel at low cost is still a frontier hot issue. Theoretically, the corrosion between LMs and Fe depends on the mutual penetration of the two elements, and

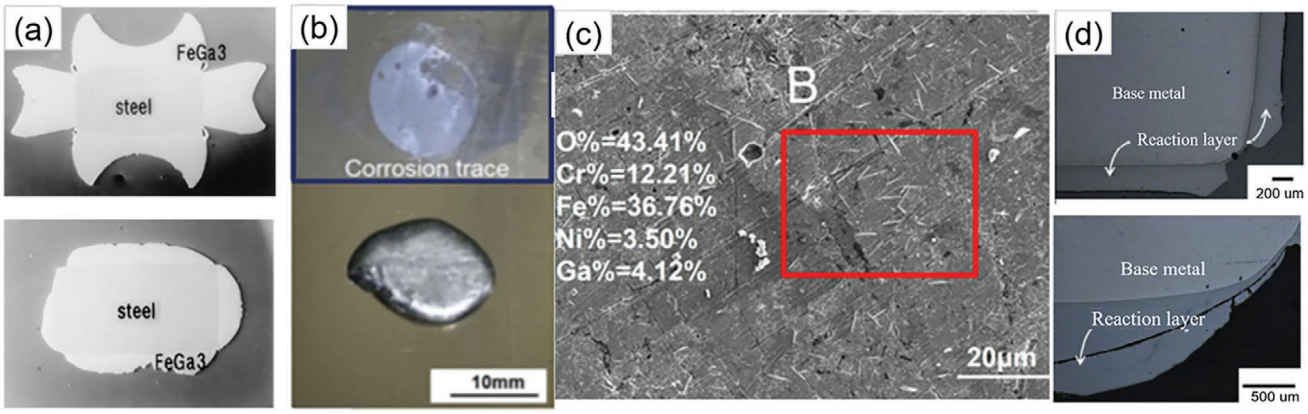

Figure 2. Corrosion characteristics of LMs and stainless steel. a) 1.4914 martensitic steel and 316 L austenitic steel specimen exposed to gallium at 400 °C for 307 h. Reproduced with permission.[49] Copyright 2005, Materials Research Society. b) Corrosion trace at 200 °C for 2 h. Reproduced with permission[28] Copyright 2018, Springer. c) Morphologies and EDS results of corrosion surfaces and cross section of 304 stainless steel. Reproduced with permission.[28] Copyright 2018, Springer. d) Optical images of specimens after exposure to liquid gallium at 500 °C for 17 and 700 h. Reproduced with permission.[50] Copyright 2012, Elsevier.

the use of anticorrosion coatings can effectively prevent metal corrosion.[73] Another idea is to pregenerate the $FeGa_3$ intermetallic compound infiltration layer between stainless steel and LMs to prevent corrosion. According to the binary phase diagram, when the concentration gradient of Ga or the driving force of Ga diffusion in the intermetallic compound layer is insufficient, it is difficult for Ga to continue to enter the stainless steel, which will reach a dynamic balance.[52,74] The current research in this area still needs further experimental verification.

Compared with traditional solid lubricants such as graphite, liquid lubricants have the advantages of low noise and strong durability.[75] However, the poor stability and narrow operating temperature of liquid lubricants restrict their application.[76] As a kind of liquid with good fluidity, excellent thermal conductivity, and a large liquid temperature range, LMs are ideal lubricating materials.[77,78] However, LMs are prone to corroding steel at high temperature, so it is necessary to study the performance of LMs and steel during friction. The formation of $FeGa_3$ plays a key role in applying LM lubricants in wide temperature range.[54,77,78] Li et al.[77] reported that when using gallium-based LMs as a lubricant, the argon-based LMs could provide excellent frictional lubrication over the wide temperature range of steel at –10–800 °C, mainly due to the generation $FeGa_3$ lubrication film and a high thermal diffusion rated during friction. Moreover, the friction loss was small. Guo et al.[52] prepared a 26.8 µm film of $FeGa_3$ on T91 steel shown in **Figure 3**a, which had a good effect of reducing friction. The phenomena and mechanisms of friction between argon-based LMs and T91 steel under conditions of 200–800 °C was explored.[77] The interface created by the friction between LMs and steel can provide sufficient lubricity and stability for the friction system. Researches on friction between LMs and steel prove that LMs are a kind of liquid friction agent with great potential, but they are easily oxidized in the air forming an oxide layer,[2,3,40] which is a difficulty that needs to be overcome for tribology.

2.1.2. Preparation of Magnetic Liquid Metals

The combination of LMs and Fe particles has also been reported to be capable of making a magnetohydrodynamic material. A layer of iron powder is coated on the oxide layer of the LMs surface to make a magnetic marble.[79–81] Magnetic LM fluid can be prepared by internalizing iron powder or mechanical alloying.[82] In the study by Kim et al.[79] and Jeon et al.,[42] Fe powder was adhered to the oxide skin on the surface of LMs, producing a LM marble with magnetism. In the study of Florian Carle et al.,[83] LMs and Fe powder could react in hydrochloric acid environment. Fe would be rapidly internalized by LMs to produce magnetic fluid. This method enhances the magnetism of LM droplet but also alter the rheology and other physical properties of the fluid. The magnetic LM with small amount of Fe (less than 5%) appears like a slurry with higher viscosity. Thus it has better ductility or extensiblity. Hu et al.[40] achieved large scale deformation even in 3D space under magnetic manipulation. When the Fe mass ratio increased to 42%, the mixture appeared solid. The addition of Fe also changes other physical properties of the LM. For example, Wang et al.[84] found that the magnetic LM-Fe composite presents much smaller supercooling effects compared with pure LM, which is due to the quick nucleation facilitated by the Fe nanoparticles inside. They prepared a transition-state magnetic fluid by mixing gallium and magnetic particles, which could lock the object during the reversible solid–liquid phase change process shown in Figure 3b, giving non-this object the possibility of magnetic operation.[86]The heating efficiency also increased under alternative magnetic field. In addition, micrometer LMs and Fe composites[41,85] have also been reported. Aaron Elbourne et al.[39] fabricated a micro Fe particle with LMs oxide layer coating. The micro Fe-LM particle could change its shape from small spheres into smaller particles, strips or stars by a rotating magnetic field action.

The mixture of LMs and iron particles endows LMs with magnetism. During the preparation and application process, the surface oxide layer of LMs is removed or prevented through the hydrocarbon group,[82] surfactant,[87] plastic materials,[88] and the acid or alkaline solution environment,[22,89] which allows magnetic LMs to be more widely used in fields such as drug loading,[34,72] controllable machines,[8,38,40] and electrical switches.[42,80]

2.2. The Combination of LMs and Cu

2.2.1. Corrosion between LMs and Cu

Corrosion also occurs between the LMs and copper substrates. The corrosion speed is faster than iron and it can even occur at

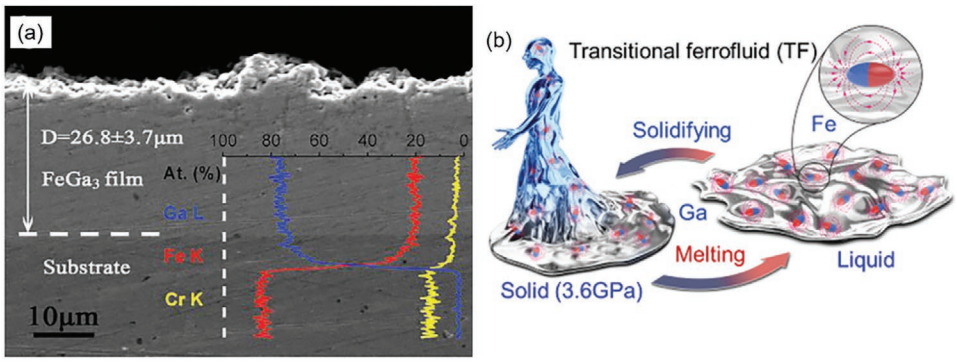

Figure 3. LMs used as lubricants and magnetofluid. a) Cross-section morphology and composition of $FeGa_3$ film. Reproduced with permission.[52] Copyright 2018, Elsevier. b) Phase change between a solid and liquid of the magnetic fluid made by Ga and Fe. Reproduced with permission.[86] Copyright 2021, Wiley-VCH.

room temperature.[55] The intermetallic compound $CuGa_2$ can quick form between gallium and copper.[51,90] In the Cui et al. study,[28] a shallow trace was left after put a LM droplet onto Cu substrate at 100 °C for 2 h. As shown in **Figure 4**a, traces deepened at 200 °C and LMs adhered to the copper substrate, the surface of LMs metallic became dull at this time. Elemental analysis indicated that the mass ratio of Ga to Cu at the corrosion interface was about 59.56%: 40.44% at region C. LMs adhered to the surface of the copper substrate at region D. Serious corrosion occurred at 400 °C, with some folds on its surface, indicating that the LMs oxidation degree became more severe. Figure 4b[55] shows the rough surface morphology of $CuGa_2$. According to this characteristic of the copper-gallium reaction, $CuGa_2$ interface materials can be prepared, and a new method of room temperature welding is proposed. Under the action of electrochemistry, the continuous flow of LM droplet precursor film can accelerate the formation of $CuGa_2$ significantly.[91] The LMs composite copper foam produced by this feature shown in Figure 4c, has stronger heat dissipation performance. Infiltration between copper and LMs was of great interest. The contact angle between LMs and copper substrates was 145° in 0.05 mol L^{-1} sodium hydroxide solution and 67° on Cu substrates with $CuGa_2$ generated after removal of the surface oxide layer of EGaIn. In 1 mol L^{-1} HCl, the contact angle of LMs on $CuGa_2$-Cu was only 11.08° due to the removal of the surface oxide layer of copper, demonstrating the superwetting performance.[91]

Because the corrosion between copper and LMs can occur at room temperature and the reaction is relatively rapid, It is unwise to encapsulate the LMs in copper. It is proved that the infiltration layer generated between copper and LMs can form an anchor point to LM and fix one side of LM, which is valuable for research on directional driving LM. Meanwhile, the obtained intermetallic compound $CuGa_2$ from the reaction between LMs and copper can be used in heat dissipation,[91] electronic welding,[55,61] and other directions.[92,93]

2.2.2. Preparation of Pasty LMs Based on Copper Powder

Tikhomirova[94] found that mixing copper powder and gallium could produce $CuGa_2$ and form a paste-like solid at room temperature. They reported the dispersing methods, newly formed compounds, and interpreted the mechanism of semisolid phase formation. Ancharova[95] investigated the reaction of copper with liquid gallium at 20 °C and found that $CuGa_2$ was the only product. Guo et al.[14] used a mixture of copper particles and LMs in a solution of sodium hydroxide to prepare Cu-EGaIn hybrids. The physical properties such as fluidity, texture, and electrical conductivity of the composites prepared with a copper mass ratio of 0–20% were studied. Through the improvement of the preparation methods, the thermal conductivity of the prepared composite material increased by 180% by mixing Cu nanopowder with LMs in an oxygen-free environment to reduce the oxidation of LMs. This is because the efficient thermal channel is created by the nanoparticle clusters.[96] With the heavier mass of the copper particles, its fluidity was decreased, but the electrical conductivity was improved. Shu et al.[97] stirred LMs and copper particles in HCl solution, which could remove the oxide layer on the surface of both LMs and copper particles. After the copper and LMs were fully infiltrated, the mixture would lose fluidity and formed a particle-based material, the main composition of which was copper and copper-gallium alloy. Tang et al.[98,99] found that copper particles could be infiltrated and engulfed by LMs in acidic solution. A similar experimental effect could be achieved by applying an electrical potential to a neutral solution, which was also owing to the removal of LMs oxide layer under the above three conditions. The combination of LMs and copper powder can change the tension, fluidity, viscosity, and other properties of LMs and enhance the plasticity of LMs, making the material easier to process and shape.

2.3. The Combination of LMs and Other Transition Metals

Since metals such as iron and copper have been widely used in industry and our daily life, the corrosion of LMs and copper or iron has become a serious problem that needs to be resolved. Thus the studies between LMs and copper or iron are mainly based on metal block and plate. While silver and gold are difficult to contact LMs in the form of block or plate, so the metal foil or film are applied to mixing. Dropping liquid Ga on the silver film, the liquid Ga would diffuse forward along the silver,

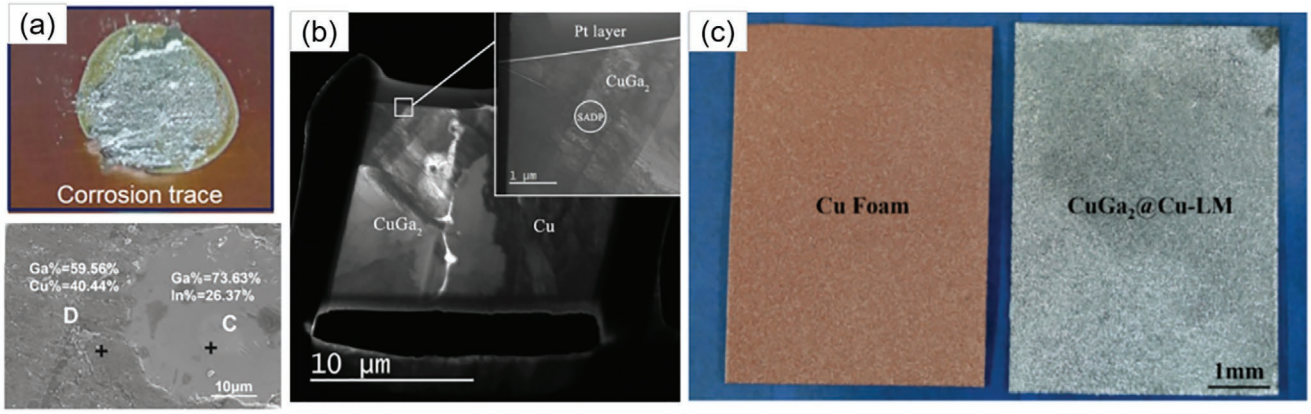

Figure 4. Corrosion characteristics of LMs and 2 copper substrates. a) Corrosion at 200 °C for 2 h without corrosion. Reproduced with permission.[28] Copyright 2018, Elsevier. b) TEM of $CuGa_2$. Reproduced with permission.[55] Copyright 2019, Springer. c) Optical photo of copper foam infiltrated by LMs. Reproduced with permission.[91] Copyright 2018, Royal Society of Chemistry.

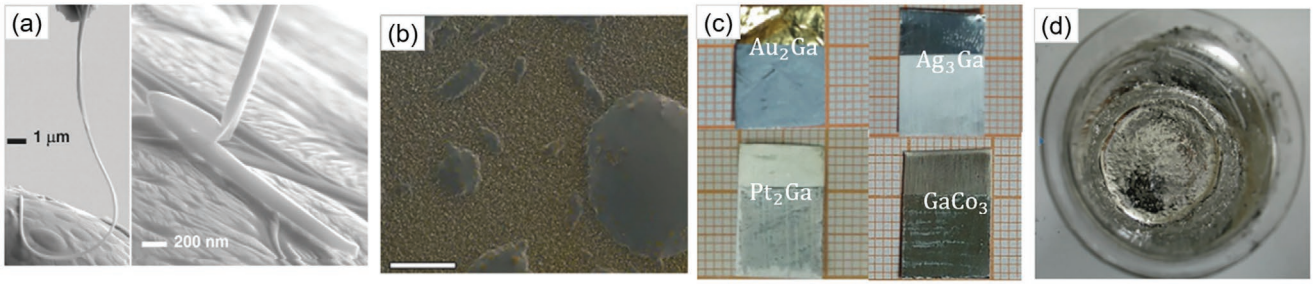

Figure 5. The combination of LMs and other metals: a) Scanning electron microscope (SEM) diagram of elastic deformation of $AgGa_2$ needle. Reproduced with permission.[67] Copyright 2005, AIP. b) Liquid Ga deposited on gold to form alloy $AuGa_2$. Reproduced with permission.[68] Copyright 2016, Wiley-VCH. c) Au, Ag, Pt, and Co corroded by Liquid Ga at 100–150 °C for 5–10 h. Reproduced with permission.[53] Copyright 2018, Royal Society of Chemistry. d) LMs and nickel particles mixed into a mud-like substance. Reproduced with permission.[92] Copyright 2019, Wiley-VCH.

which was not a common wetting phenomenon but generated alloy compounds and Ag_2Ga.[67] The reaction between silver and liquid Ga is fast. Yazdanpanah[67] inserted the silver-plated film into the liquid Ga, Ag_2Ga could be observed after 2 min, with a shape of needle. This needle could deform plastically, as shown in **Figure 5**a. Unexpectedly, the needle was not strongly infiltrated with LMs, which was different from the combination between copper and LM. It was revealed that the silver film was dissolved into particles by the action of Ga and then combined with Ga atoms to recombine into Ag_2Ga crystals. Owing to the high bonding of silver and LM,[100] low-cost hydrophilic-based LMs microcircuit printing technology can be realized. By inkjet printing water-based nanosilver ink on the polyvinyl alcohol substrate, and then printing a layer of LMs, the electrical conductivity and stretchability of the circuit was greatly increased. Ag was a strong anchor of In,[101] and In had a strong binding ability to gallium, so LMs were tightly adhere to the inkjet Ag.[102]

$AuGa_2$ alloy can be generated on the gold foil with Ga evaporated, which can reduce the surface tension of LMs to form a continuous pattern in Figure 5b.[68] Liquid gallium was applied on the gold foil reacted for 5 h at 100 °C, as shown in Figure 5c, the original LMs metallic luster turned into a cyan substance, which was detected to be $AuGa_2$ by XRD. The phenomena and products of Ag, Pt, and Co under the corrosion of Ga were also studied and described in Figure 5c.[53]

Nickel can be corroded by LMs at a low speed. A corrosion layer thickness of 50 μm could be seen at 220 °C after 300 h in **Figure 6**f. The thickness and weight of the reaction layer increased with the corrosion time. The weight of the Ni block increased 70% after 1200 h,[103] it could be judged that the corrosion was alloying process according to the increase of reaction layer and Ni block mass. In the study by Ma Biao et al.,[92] Ni was combined with LMs as a magnetic material to prepare magnetic fluids shown in Figure 5d. Ni particles could also be used to modify LM. Slight oxidation can reduce the surface tension of LMs and improve the ability of LMs to bind with other materials by infiltration, in which case LMs bind more easily with other materials. In Xiong et al.'s study,[104] they mixed Ni particles with LMs to prepare magnetic LMs, and notably, they precoated Ni particles with SiO_2 so that Ni could be dispersed in LMs more evenly. During the fabrication process, Ni was mixed with LMs in air, which resulted in an increasing degree of oxidation of the LMs, while the ability to bind and disperse with Ni was enhanced. Guo et al.[14,20,103] investigated the properties, mobility, and conductivity differences of different Ni particle mass percentages (0–20%) after addition of LM. The larger the Ni particle mass percentages were, the less conductive and less mobile the LMs would be. Zhang[72] et al. used electroplating Nickel salt solution to form a thin nickel cap covering on LM. Peculiarly, LMs can hardly corrode with Ti, so NiTi alloys cannot be corroded by Ga at low temperatures, mainly because of the stable chemical structure of NiTi alloys.

Because of the strong electronegativity of Ga in LMs, chemically and theoretically, Ga can displace Au, Pt, Cu, and other less active metals from solutions.[24,26,105] Thus LMs can be used to produce metals from waste water. The study of David et al.[24] suggests the pH could influence the reaction phenomena. Respectively, it could be seen that a thick black shell was formed in acidic solutions, a thin layer and a few black spots were formed in neutral conditions, while in alkaline generates there was a thin film-like gold structure. The thickness and quality of the generated layer of gold nanoparticles could be controlled by regulating the concentration, pH, and other conditions of the reactants. When the solution environment was acidic, the LMs surface oxidation layer would be removed, at this time the restored copper particles would be infiltrated by LM. At the same time, Ga would also react with H^+ to generate hydrogen. LMs tend to form galvanic battery corrosion with the substituted metal, but in some experimental studies, no corrosion occurred, which is attributed to the fact that LMs oxide layer surface is very easy to form.[89] The main component of the oxide layer is Ga_2O_3, with relatively stable chemically and lower surface tension, plays a role in protecting the LM.

The phenomenon of the combination of LMs and metal mainly includes the corrosion of LMs and TMs, the combination of LMs and various TMs particles, the combination of LMs as a reducing agent to replace TMs and producting composite materials using the LMs as a liquid platform. Among them, some intermetallic compounds can be formed after LMs and TM are corroded, which largely depends on the mutual solubility and eutectic relationship between various metal elements. The reference data for the multicomponent liquid eutectic system is limited.[101] The reaction of LMs and other metals is mainly corrosion and infiltration.[2,51] Using the interaction of LMs and these metals to realize the repair

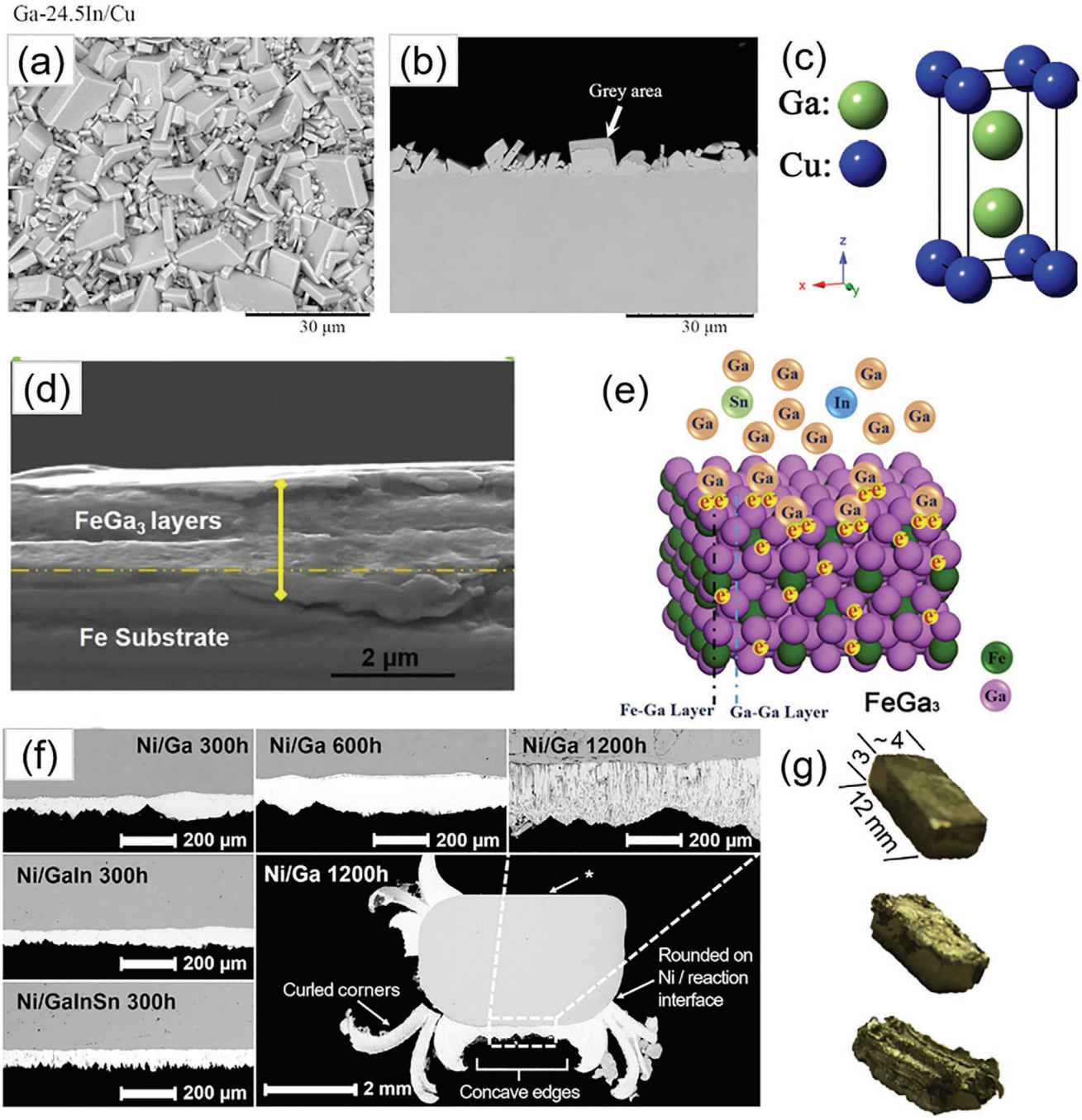

Figure 6. LMs and different metal corrosion morphology and atomic configuration. a) LM and Cu corroded SEM backscattered electron images, b) Side view of a). Reproduced with permission.[55] Copyright 2019, Springer. c) The atomic configuration of $CuGa_2$. Reproduced with permission.[92] Copyright 2019, Wiley-VCH. d) Fe and LMs corroded to generate the cross section of $FeGa_3$ interface. Reproduced with permission.[59] Copyright 2019, Elsevier. e) $FeGa_3$ schematic diagram of interface wetting model. Reproduced with permission.[59] Copyright 2019, Elsevier. f) SEM images of Ni and LMs sections corroded at 220 °C. Reproduced with permission.[103] Copyright 2020, Elsevier. g) Morphology of Ni and LMs corroded at 220 °C for 300, 600, and 1200 h. Reproduced with permission.[103] Copyright 2019, Elsevier.

of circuits,[85,106] the design of flexible electronic printing materials,[14,16,31] smart switches,[42,107] and other applications,[108] making the researches of LMs diverse and exciting. It is meaningful for the controllability of the research processes,[26] the recycling of materials, and the expansion of interactive applications.

3. Mechanism of the Combination of LMs and TMs

The mechanism of corrosion, substitution, wetting, and other phenomena caused by the combination of LMs and TMs are discussed in this section. The relatively high chemical activity

of gallium is the main reason for its corrosion and substitution when electrochemical interactions take place. The formation of intermetallic compounds should be responsible for the wetting and adhesion behavior.[28] The phase composition of the alloy can be judged with the help of the metal phase diagram.[109] The properties of alloy crystals are determined by the interaction between molecules, atoms, and electrons.[110] The structural characteristics of the crystals can be observed and studied by X-ray diffraction,[5,67] electron microscopes,[111] etc. When LMs are contacted with a solid metal interface,[112–115] the study on the wettability and interface is important, which can be described by the contact angle[116] and Laplace–Young equation.[117]

3.1. Alloying Corrosion

The corrosion process of LMs and TMs is a complex process, including the dissolution, mass transport, chemical reaction, new phase formation, and oxidation processes. Refractory metals (such as tungsten) will not form intermetallic compounds with LM.[118] Specifically, it can be explained as the material transportation of LMs in solid-phase metal, the dissolution of solid-phase metal in LMs, and the complex reaction at the interface.[119] The transport of corrosion products in the solid and liquid phases and the dissolution reaction at the interface determine whether the surface structure of the solid metal would be destroyed. The mechanism of LMs corrosion can be described and explained by the mass transfer equation of material conservation: $\frac{\partial c}{\partial t}+\nabla J+q=0$, where c is the mass concentration, J is the diffusion flux, and q is the reaction consumption[120] term. Studying the corrosion mechanism of LMs and other transition metals is a complex and interdisciplinary research direction, which has an active guiding role in the application of LMs in thermal management,[78] aerospace,[121] medical devices,[34,51] and electronic equipment.[62,122]

Fe, Cu, Ag, Au, Ni, Pt, Co, etc., will all undergo alloying corrosion by LM.[58,104,123] LMs and copper are corroded to produce $CuGa_2$. In the study of Liu et al.,[55] it was found that when Ga and Cu reacted, an uneven copper interface appeared on the Cu surface, and $CuGa_2$ was formed on the uneven interface. Figure 6a displays a crystal electron microscope image of $CuGa_2$, and Figure 6b shows an alloy layer. The element content diagram shows that the Cu:Ga mass percentage of the alloy layer is about 1:2, and the Cu interface is uneven, which suggests that the dissolution rate of Cu atoms in some positions is faster than in other positions. Lin et al.[62] studied the phase transition kinetics, reaction mechanism, and microstructure changes of the contact reaction between copper and gallium at 160–300 °C. $CuGa_2$ has a square layered structure in the P4/mmm space group, and the crystal parameters are a = 2.8301 and c = 5.8294. This layer unit consists of the internal sharing of two Ga atoms in the Ga layer. At room temperature, the crystal grains formed by Cu and Ga are 10–20 μm long and 5–10 μm thick. The projection diagram of the unit cell and crystal structure of $CuGa_2$ is shown in Figure 6c.[92] In the martensite 1.4914 experiment,[49] the dynamic growth showed a cross shape and a concave shape, with a linear growth law, which indicates that the corrosion process was mainly controlled by the interface law. In the austenite 316 experiment, the dynamic growth changed from the cross shape to the convex shape, with a parabolic growth law, which indicates that the corrosion process was mainly controlled by the diffusion law. Figure 6d shows the corrosion of Fe after 30 min, and it can be seen that an alloy layer of about 2 μm thickness was formed.[59] Lue et al.[124] reported that $FeGa_3$ was a tetragonal $CoGa_3$-type structure with a space group symmetry of P 4_2 /mnm. It was a semiconductor, and its lattice parameters were a = 0.6251 and c = 0.6543 nm, respectively. The schematic diagram of the crystal structure is shown in Figure 6e,[59] the upper layer is Fe-Ga and the lower layer is Ga-Ga. At 273 k, the conductivity of $FeGa_3$ is about 5 mΩ cm^{-1},[124] which increases with increasing temperature.

Corrosion of silver by LMs produces Ag_2Ga. Ag_2Ga is a hexagonal crystal system with a noncentrosymmetric space group P62m.[67] The lattice parameter a = 0.77 680 nm, c = 0.28 759 nm.[125] The reaction between silver and liquid Ga is fast. In the study of Yazdanpanah et al., inserting a silver-plated needle into liquid Ga,[67] Ag_2Ga can be seen to be formed in 2 min and form a needle shape, which has been introduced in Section 2.

Ni and LMs are corroded at 220 °C to produce Ni_2Ga_3 and Ni_3Ga_7.[103] The fine needle-like phase morphology can be observed on the sample. This is the characteristic of interface-dominated diffusion. According to the experimental EDS, Ga is in the Ni lattice. In Figure 6f, we can observe the corrosion state of Ni in gallium, gallium indium alloy, and gallium indium tin alloy.[104] Figure 6g shows the corrosion of Ga and Ni over time. At the same time, we can conclude that the principle of Ni and Ga corrosion is similar to that of Ag. The mechanism of nickel gallium corrosion is that Ni dissolves into the LMs and eventually reacts with LMs. At room temperature, the mixing of Ni nanoparticles and LMs will generate intermetallic compound Ga_4Ni_3.[126]

The combination of Au, Pd, Pt, Co with LMs will generate $AuGa_2$, fcc Pd (Ga) solid solution alloy,[127] Ga_2Pt,[26] and $CoGa_3$ respectively. Norkett et al.[128] summarized the factors and mechanisms of LMs embrittlement, including interface cracking, intergranular penetration and LMs corrosion, and also proposed the corrosion mitigation measures such as adding alloys and coating processes, which have great importance for the study of LMs and TMs combination. It is possible that Ga can dissolve into other metals to form alloys and vice versa. The reaction rate is controlled by diffusion or interface law.[119,129] The mechanism behind this needs to be further studied.

3.2. Replacement Mechanism

Section 2.3 has discussed the characteristics of LMs replacing Cu, Au, Pt, etc., from solutions. This section summarizes the principal research of LMs electrochemical replacement of other metals. Ga^0 /Ga^{3+} (ε = –0.529 V), the potential is low, theoretically it can be electrochemically replaced with a higher potential solution. In the study of Chen et al.,[105] Cu was replaced by LMs from acidic $CuSO_4$. Through the analysis of element concentration changes before and after the reaction, the chemical

reaction formula was $3Cu^{2+} + 3Ga = 2Ga^{3+} + 3Cu$.[112] In this reaction, the primary battery Cu for the anode, hydrogen gas is generated, and Cu particles are generated at the cathode Ga. It is not obvious when HCl is not added. This is because the LMs in the solution will preferentially form the oxide layer Ga_2O_3, and the Gibbs free energy of Ga_2O_3 is higher. In the displacement reaction, the precursor interface materials will affect the mechanism and reaction process of the displacement reaction. The presence and absence of an oxide layer on the surface of the LMs have a huge impact on the experimental results.[25]

In Faegheh Hoshyargar's research,[130] they found that Ag and Au could be replaced by LMs, and the experimental phenomenon was shown in **Figure 7**a, the surface of the LMs was covered with replaced Au or Ag after 24 h. Figure 7b describes the influence of time and concentration to the replacement reaction in $KAuBr_4$ with neutral pH.[25] Figure 7c quantitatively describes the change in the percentage of substituted gold and reduced gallium over time. When LMs replace gold in a $KAuBr_4$ solution with a pH greater than 11.7, the potential of $AuBr_4^-$/Au is 0.854 V, and the equation for replacing gallium with LMs is $Ga + AuBr_4^- \rightarrow Ga^{3+} + Au + 4Br^-$,as shown in Figure 7d. At pH 3–11.7, the surface oxide layer of LMs Ga_2O_3 can stably exist in the solution, so after the replacement reaction, $Ga3^+$ continues to react, $Ga^{3+} + 3H_2O \rightarrow Ga_2O_3 + 6H^+$. When the pH is higher than 11.7, there is $Ga_2O^{3+}3H_2O \rightarrow 2GaO^{3-} + 6H^+$.That is to say, when the pH > 11.7, the reaction environment will inhibit the initial oxidation of the LMs, and it can also inhibit the reformation of the oxidation product during the displacement reaction. Olawale Oloyeyan[56] studied how LMs replace Pt at room temperature. It is worth noting that after the replacement

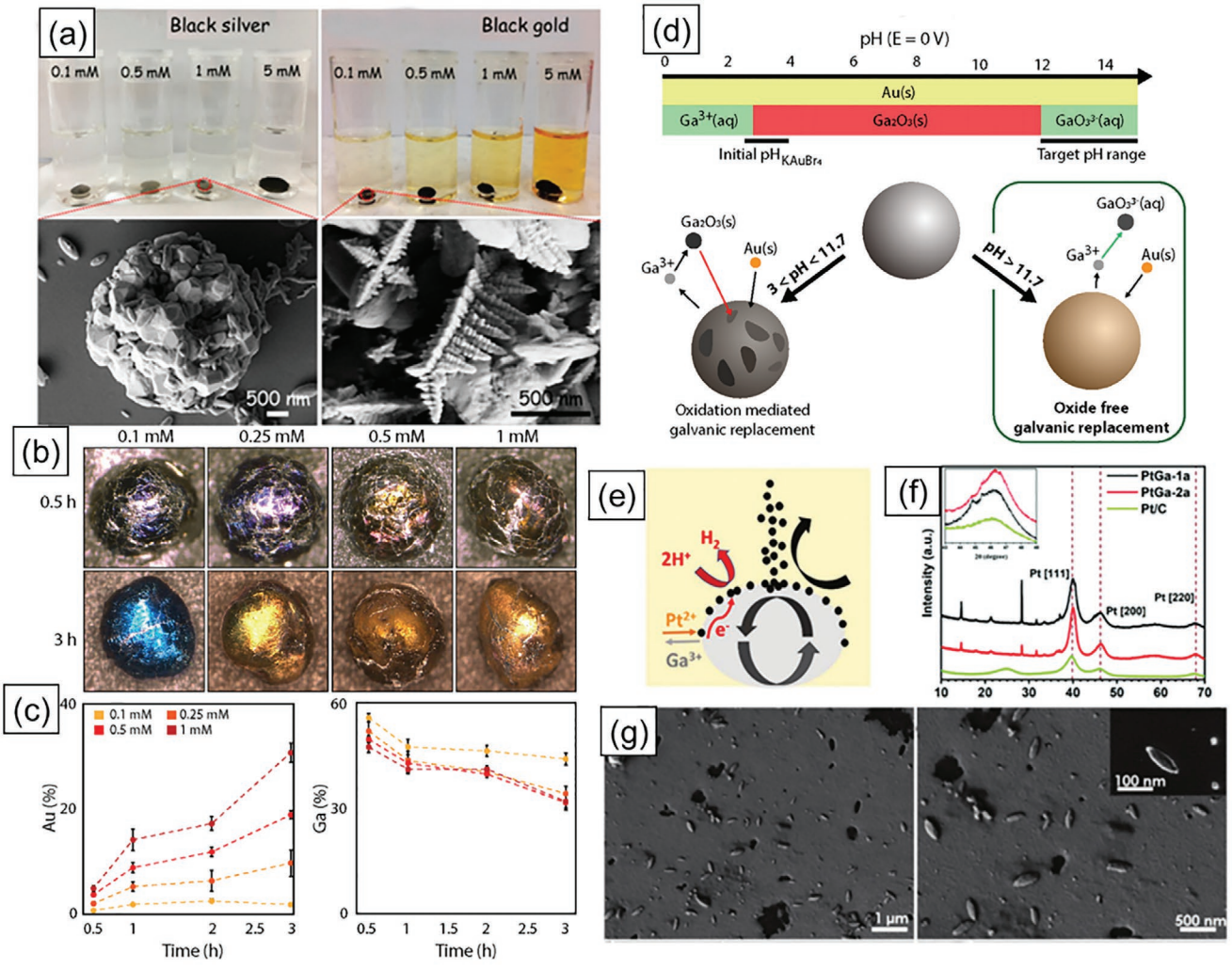

Figure 7. Mechanism of LMs electrochemical replacement TMs and subsequent reaction, a) Ag replaced in $AgNO_3$ after 72 h and Au replaced in $KAuBr_4$ after 24 h of different concentrations by LMs. Reproduced with permission.[130] Copyright 2017, ACS. b) Optical photographs of LMs replacement Ag in neutral $KAuBr_4$ solution at different time and concentrations. Reproduced with permission.[25] Copyright 2018, ACS. c) The percentage of Ga and Au in the reaction–time relation curve of b). Reproduced with permission.[25] Copyright 2018, ACS. d) The mechanism of Ga_2O_3 on the electrochemical reaction of Ga replacing Au in different pH solutions, Reproduced with permission.[25] Copyright 2018, ACS. e) Electrochemical principle of LMs replacing Pt in K_2PtCl_4. Reproduced with permission.[23] Copyright 2019, Royal Society of Chemistry. f) XRD of Products under neutral and acidic conditions. Reproduced with permission.[23] Copyright 2019, Royal Society of Chemistry. g) SEM pattern of Pt generated by replacement in neutral 7×10^{-3} M K_2PtCl_4 condition. Reproduced with permission.[23] Copyright 2019, Royal Society of Chemistry.

reaction occurred, the electrons released from the galvanic cell would be transferred to the displaced Pt, and under the catalytic action of Pt, H^+ would be reduced to hydrogen released from the solution, depicted in Figure 7e.[23] Figure 7f,g described the micromorphology and elemental analysis of the product Pt. In addition, Kumar et al.[131] used ultrasound to produce gallium particles, and used gallium particles to replace $AgNO_3$ solution, $CuSO_4$ solution, $HAuCl_4$ solution and Zn $(CH_3COO)_2$ solution at 25–50 °C. Among them, Ag, Cu, Au can be replaced, but Zn cannot be replaced as Zn has stronger electronegativity than Ga. The replaced Ag, Cu, and Au combine with Ga to form Ag_2Ga, $CuGa_2$, and $AuGa_2$.

3.3. Interfacial Mechanism

A thin solid oxide layer is easily formed on the surface of LMs in a micro-oxygen environment. This oxide layer has a certain mechanical force and the critical surface yield stress is about 0.5 N m^{-1}, which can support a certain amount of LMs droplets keep a certain shape, and the thickness of the oxide layer is about 3 nm.[132] When LMs have an oxide layer, the wettability is affected by the surface roughness of the metal solid.[114,115] The oxide layer of LMs can be removed by applying voltage or by acid or alkali.[72,89] When removing the oxide layer on the surface of the LMs, the contact between the LMs and the metal can have both wetting and nonwetting performances. LMs can infiltrate with copper, gold, silver, etc., when removing the oxide layer.[62,67] Because of the controllability of the oxide layer on the surface of the LMs, the formation or removal of the oxide layer on the surface of the LMs changes the surface tension, which can change the interfacial characteristics of the LMs and other metals. This dynamic solid–liquid interface characteristic can provide a good research platform for interface science theory. It is worth noting that after the LMs and the metal contact and infiltrate, if there is an oxide layer on the surface of the LMs,[133] this oxide layer may be destroyed under the final embrittlement, so the internal LMs will quickly diffuse on the solid metal surface.[129,134,135] In the study of Jin-Lei et al.,[91] they connected an external current to the copper substrate to induce a continuous flow of LMs on the copper substrate, accelerate the formation of $CuGa_2$, and form a reactive wetting coating on the interface between the LMs and the copper. LMs were placed on the copper foil base connected to the negative electrode, and the sodium hydroxide solution was connected to the positive electrode. Under the action of voltage, it moved from left to right at a speed of about 3.5 mm s^{-1}. It was interesting to find that the head moved forward, the tail remained at the left end. After washing away the LMs, a layer of silver-white material remained on the copper surface, which was tested to be $CuGa_2$. The principle of directional movement is that the LMs forms a $CuGa_2$ precursor film on the copper, and the $CuGa_2$ interface energy is lower under the action of voltage, resulting in directional movement of the LM. $CuGa_2$ has super wettability with LM. The mechanism of super wettability is that the generated $CuGa_2$ provides a stable metal bond to induce wetting behavior: the work function of $CuGa_2$ is about 4.47 eV, which is very close to the work function of pure liquid Ga (4.32 eV), which is the difference between Ga and $CuGa_2$.[51] The valence electrons can be exchanged easily, leading to strong valence electron hybridization and metal bonding, and the macroscopic effect is reflected in the superwetting performance.

LM can also be reactively infiltrated on the Fe surface, because Fe and Ga can form $FeGa_3$ intermetallic compounds. On this compound, the contact angle of EGaIn with Fe substrate in 1 mol L^{-1} HCl is only 35.02°. The $FeGa_3$ iron substrate has a contact angle of 73.62°. The reason for this change is believed to be caused by the interaction of metal bonds.[59] Cui et al.[51] established the LGAs-$FeGa_3$ model. By drawing the electron localization function diagram (ELF) and the crystal structure, they believed that the valence electron hybridization between Ga—Ga and Ga—Fe atoms was the reason for the formation of this metal bond. The wetness and metal bond interaction have similar trends with the adsorption energy, which is proved by first principles. What's more, they used experimental methods to measure the adsorption force, and the calculated adsorption energy was consistent with the simulation results.

The oxide layer of the LMs changes the wettability of the LM. The surface tension of the LMs decreases sharply from 624 mN m^{-1}.[34] The oxide layer on the surface of the LMs has a certain viscosity and oxide shell layer can adhere to almost any surface. It means that when there is an oxide layer, it can be easily combined with other materials, and it can stick Fe powder, Ni powder, etc., on the surface of the oxide layer. When the LMs are stirred in the air, a mud-like solid can finally be obtained.[136] In this process, other powdery materials can be added to modify the LM. Tang et al. have studied this aspect.[98,99] When the transition metal powder and LMs are mixed in the air, a mud-like substance is also formed. Because other metals are added, their physical and chemical properties will change. It will not be reported in detail here. The mechanism is due to the oxidation of the LM. The layer is viscous and acts as a combination of powder materials. At the same time, stirring the LMs in the air will accelerate the oxidation of the LM.

4. Applications

The flexibility and conductivity of LMs make LMs to be widely applied in the field of flexible devices and microelectronics,[87,137,138] but its high surface tension, oxidized characteristics, and poor stability bring difficulties in its further applications.[139] Combining LMs with TMs, such as copper powder, nickel powder, and iron powder is able to solve the above problems of LMs, which present attractive properties. In particular, the micro-nano manufacturing of LMs, due to the size effect, has given LMs more possibilities in biomedicine, catalytic engineering, and other fields.[140,141] In this part, we discussed the applications of the combination of LMs and transition metal in three directions: electronic devices, multifunctional materials, and medical applications.

4.1. Applications in the Direction of Electronics

LMs have been widely applied in stretchable electronic devices due to its excellent electrical conductivity and flexibility. On the

one hand, it has better flexibility and good ductility than traditional iron, copper, and gold. On the other hand, as a flexible conductive material, it has better conductivity than hydrogels and polymer organic conductive materials. These advantages make LMs have a more excellent application range in electronic devices, flexible sensors, and other directions. The combination of LMs and other metals can further improve the viscosity, conductivity, and plasticity of the material under the condition of ensuring the flexibility and fluidity of the LMs.

Due to its good wettability with metals, LMs and highly conductive metals such as silver, gold, and copper can be made into highly conductive flexible materials for island-bridge structures and core–shell structures shown in **Figure 8**a. The island-bridge structure originated from the thick-film deposition process used to fabricate stretchable electrochemical devices.[142] Wrapped in a flexible substrate, the oxide layer of LMs particles squeezed is broken, and the LMs with wettability and conductivity flows out of the shell and connects the adjacent silver flakes in Figure 8b.[143] The flexible conductive material exhibits similar stretchability (1000%) as the hydrogel while exhibiting high conductivity. The nickel nanoparticles are mixed with LMs, and the intermetallic compound layer formed around Ga_4Ni_3 and $InNi_3$ provides strong adhesion.[126] LMs act as a retractable bridge between solid metallic particles to provide dynamic and strong electrical anchoring. This structure provides good conductivity under high strain.[144] Wang et al. produced a flexible sensor that combines the above conductive structure with different sensing active materials.[145]

LM particle-based conductive ink is widely used in flexible device materials. The functional shell structure made of highly conductive metal is an effective way to achieve the stability and functionalization of LM particles. LM particles with a silver shell have high initial conductivity, without oxide shell. The silver shell ruptures under external pressure, and the electrical function can repair itself within 200 ms.[146] The Ag shells were fabricated by in situ chemical plating. The LM particles of the core–shell structure composed of the Au shell (Figure 8c) generated by the substitution reaction and the Cu shell[98] formed by coating the nanoparticles have similar good conductive properties.

Without combining with flexible substrates, Ag nanoparticles can be directly mixed with LMPs to make printing ink. Based on these composites, the prepared circuit has self-healing capability and high conductivity of 2×10^6 S m^{-1}.[147] The silver nanoparticles interact with the liquid alloy to form a heterogeneous substance (Figure 8d) surrounded by AgNP-In-Ga clusters and Ga-rich films. Thin-film electronic circuits printed with such composite conductive inks have excellent conductivity and stretchability.[148] Ma et al.[149] studied the sputtering of gold, silver, and platinum on the LMP, and found that the platinum-coated LMP can be used as a micro-nano motor. The micromotors composed of LMs and platinum can move along the silver nanowires when they touch in acid vapor. They fix and microweld silver nanowires to build electrical paths when they encounter connection points shown in Figure 8e. Mixed copper LMs change the original mechanical properties and adhesion, enhance electrical conductivity, and significantly

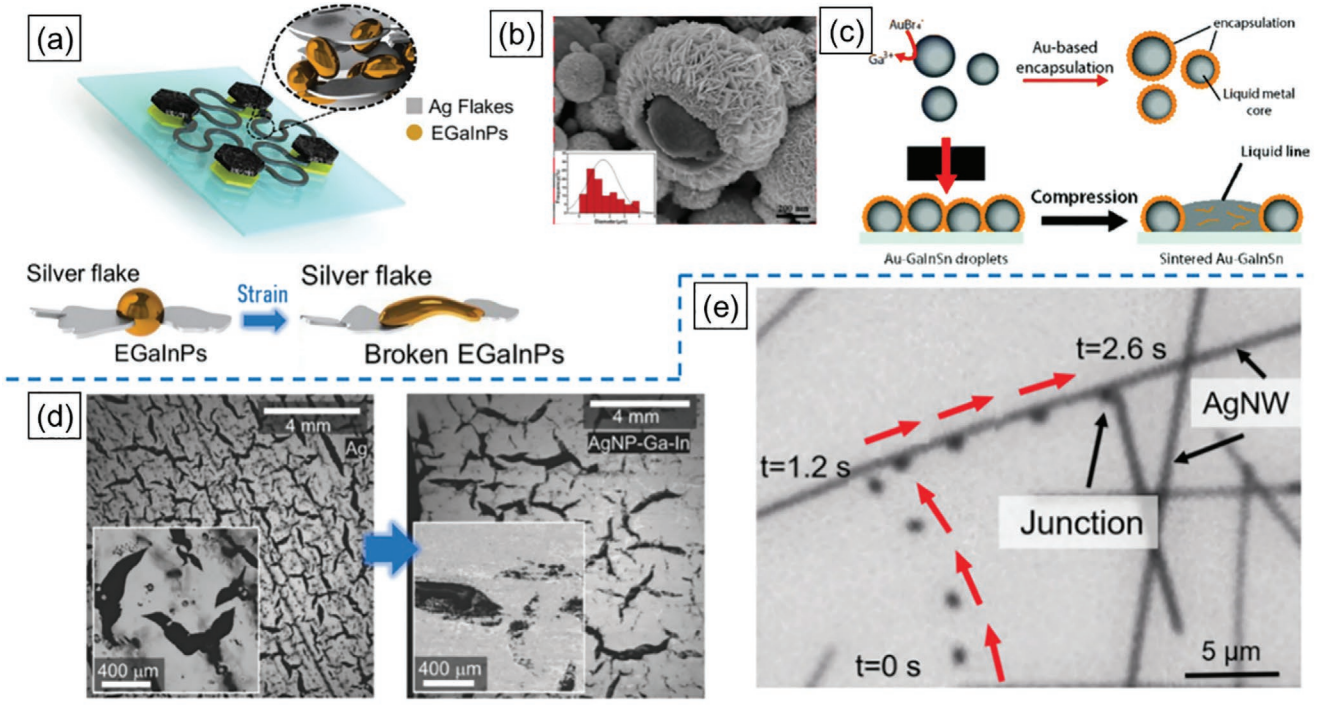

Figure 8. LMs are used in electronic welding and electronic devices. a) Island bridge structure, stretched state and electrical connection retention. Reproduced with permission.[142] Copyright 2020, Wiley-VCH. b) SEM image of LM wrapped in silver shell. Reproduced with permission.[146] Copyright 2020, Wiley-VCH. c) Schematic diagram of gold-liquid metal core–shell structure. Reproduced with permission.[24] Copyright 2019, Royal Society of Chemistry. d) Using LM to reduce the crack density of printed silver nanoparticle circuits. Reproduced with permission.[148] Copyright 2018, Wiley-VCH. e) Microwelding of silver nanowires with LM droplets. Reproduced with permission.[149] Copyright 2019, Wiley-VCH.

improve thermal conductivity. Tang et al. tested and analyzed that the electrical conductivity and thermal conductivity are directly related to the content of the mesophase $CuGa_2$.[98] Simultaneously, its excellent adhesion allows it to be used for direct writing and printing.

Based on the wettability and adhesion of LMs and ferromagnetic metal particles, researches on magnetic manipulation of LMs have made a lot of new progress in recent years. The magnetic LMs made of mechanically stirring nickel particles and LMs can be directly patterned using a magnetic field.[92] Nickel-based LMs conductive ink can control adhesion by controlling the doping ratio.[20] Nickel and LMs in the acid solution will not wet but form the primary battery, generating bubbles. The bubbles form a van der Waals bridge between them. This mechanism can also be applied to magnetically manipulated LMs to control the conduction of a circuit.[85,150]

LM mixed with iron particles has similar properties and can be used to make magnetron repairable circuits. Previously, Fe-LM can realize magnetic controllable circuit switching applications in microchannels.[42] Recent researches in this area have developed the application of magnetic LM switches into 3D space,[151] and has shown that magnetic LMs can be controlled and reversible freely large-scale expansion and contraction similar to the Terminator.[40] Zhang et al.[152] mixed Cu-Fe NPs into the LMs, in which copper facilitates the suspension of particles in the LMs, which demonstrated a good result of electric and magnetic coactuation of the LM. Wang et al.[84] demonstrated that another expansion ability of magnetic LMs heating in a solution. The spontaneous chemical reaction makes LMs become a porous, light-weight soft material. In order to achieve unique reconfigurable magnetic polarity, stiffening effect, transformed shape, and high electrical conductivity, He et al. used NdFeB to make ferromagnetic LM.[153]

4.2. Applications in Multifunctional Materials

The chemical properties of LMs are relatively active, with a certain degree of reducibility, which can reduce some metals. This property can be used to prepare multifunctional materials, especially nanopowders and membrane materials. The adhesiveness of LMs and the property of turning its liquid state into mud due to oxidation can be used to make LM-based composite materials.[154] Therefore, LMs have their unique advantages in making and designing new materials.

For catalysts, the activity and sustainability of the catalyst are important measures of catalytic performance, and the composition and structure of the catalyst affect the performance of the catalyst. In the research of heterogeneous catalysts, alloying of bimetallic elements is a research focus. LMs have reducibility, which can be used to directly prepare bimetallic catalysts.[9] At the same time, LMs have good supporting properties and can be combined with metal particles to form composite materials, which can also be combined with other metals.[132] These two properties make LMs an excellent material in the design of bimetallic catalysts. The loading of catalytic particles on the surface of LMs has been reported by many researchers. In the study of Hoshyargar et al.,[130] GaInSn was used to reduce Ag and Au to prepare composite Ag-GaInSn, and its catalytic activity was tested with methylene blue. In the report of Taccardi, N's Yanren, they loaded Pd on liquid Ga to make The Ga-rich Pd/Ga system has higher activity and selectivity.[155]

The LMs become more applicable in 3D printing by combining other metal particles to control its tension, modulus, plasticity, and viscosity. Guo et al.[14] mixed LMs and copper in different proportions and produced smart electronic clothing through a roll printing process, demonstrating the application of a low-cost wearable electronic clothing, which could work properly on the cloth with 75% straining in **Figure 9**a. Shu et al.[97] used a mixture of Cu and LMs to make a particle-based porous material with high thermal conductivity and electrical conductivity, which can be used for 3D additive manufacturing in Figure 9b. Tang et al.[98] used a mixture of LMs and Cu to fabricate metallic ink with semifluid/semisolid mechanical properties for writing circuits and 3D printing. Guo et al.[20] mixed LMs and Ni to make a flexible electronic material, and tried to make a pulse collection device using its flexibility and conductivity. Chang et al.[106] mixed LMs and Ni particles

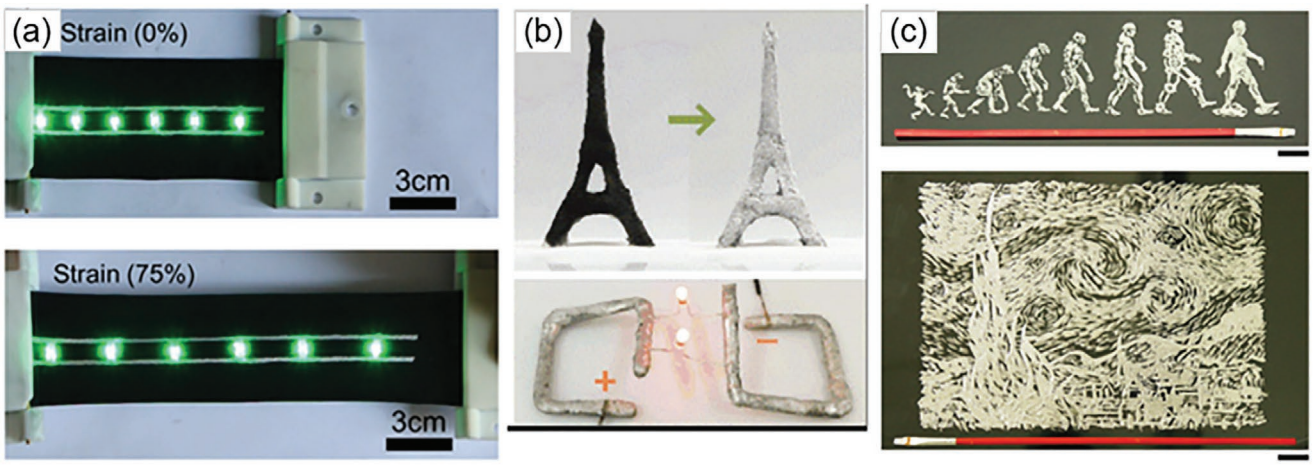

Figure 9. The applications of LMs and TMs combined in new material direction, a) Cu and LMs mixed to produce the flexible tensile conductive material. Reproduced with permission.[14] Copyright 2019, ACS. b) Cu and LMs mixed to prepare particle-based printable materials. Reproduced with permission.[97] Copyright 2020, ACS. c) Ni and LMs mixed to prepare writable metal ink. Reproduced with permission.[106] Copyright 2020, Wiley-VCH.

to make conductive ink that can be written directly on paper shown in Figure 9c. Using its plasticity, electrical conductivity, and tensile property, flexible wearable sensors can be prepared for pulse detection.

Preparing nanometal materials by LMs phase separation technology is a very promising technology. Compared with the solid interface, the liquid interface has fluidity and fracture-recovery characteristics, and the surface tension of the LMs is adjustable, which makes it possible to generate and discharge nanomaterials from LMs. Mayyas et al.[156] reported a new method for separating alloying elements in LMs based on pulse method. LMs were applied with pulse current to prepare nano-ZnO, Sn, and In. The use of redox electricity to control the surface tension of the LMs allows the elements in the liquid alloy to dissolve and separate, which inspires new ideas for the preparation of 2D materials. Ultrasound is a common method to break LMs droplets. Idrus-Saidi et al.[157] used ultrasound to destroy the liquid interface and release the elements in LMs to prepare gallium-based composite nanomaterials. They explored the size and composition ratio of materials in different solvents. It has been successfully applied to gas sensors. This method is suitable for the preparation of more composite materials combining TMs and LMs. LMs can form an ultrathin oxide layer in an aerobic environment, which can be easily pilled off. Thus ultrathin 2D materials can be prepared using this feature.[158] When TMs are added in LMs as solute, atomically thin metal oxides can be separated by bubble method or adhesion method.[133] It is worth noting that the environmental parameters for preparing these materials need to be further studied. Many products are oxidized during the formation process, or the structure is uncontrollable. In the future, it is extremely important to optimize the reaction conditions such as temperature, catalyst, and solvent environment for the preparation of industrialized and functional materials.

The reducibility of LMs offers promising strategies in designing and preparing new materials. It is known that LMs can replace less active metals such as Cu, Pd, Au, Ag, etc. Au framework pattern produced by LMs could be structurally and chemically stable in ambient air.[24] The control of the temperature, concentration, and other conditions of the substitution reaction can influence the structure and properties of the prepared material, which has a great effect on the development and application of new materials.

4.3. Applications in Medical Therapy

The unique properties of LM's flexibility, fluidity, repairability, biocompatibility make it possible to be used in the medical field. Combining LMs with other metals can achieve functions such as drug loading,[29,72] sterilization,[39] and hyperthermia.[43,159] In the study of Elbourne et al.,[39] they used the combination of LMs and Fe to produce a magnetic LMs particle that can deform in a low-speed rotating magnetic field, destroy the bacterial biofilm, and make the bacterial cell. It was the physical destruction that achieved bactericidal effect. *P. aeruginosa* cells and *S. aureus* cells were killed by the compound in **Figure 10**a. In the research of Hou et al.,[43] they used the combination of the Cu and LMs to produce a new material with the ability of low temperature ablation, which can be used for photothermal therapy for the treatment of melanoma. First, LMs and copper particles are internalized to make a paste material, which has high thermal conductivity and can completely cover the tumor site for cryoablation treatment shown in Figure 10b. The modified paste is made into nanoparticles under ultrasonic conditions, and the photothermal conversion efficiency can reach 28.8%, which can be used for photothermal treatment of melanoma. In the biosafety evaluation, C8161 cells were cultured in a solution containing paste and nanoparticles, and the cell survival rate was above 90%, indicating that the toxicity was low. It is more important that copper was not detected in the solution but only gallium and indium, and the concentration is safe to be used in the human body. This shows that after the LMs internalize the copper, it is difficult for the copper element to escape from the LMs. This study may provide a strategy to reduce the toxicity of copper so that it can be used in the human body. The Au-LM nanolitchi-shaped heterogeneous material obtained by replacing Au with nano LM has excellent thermal stability and is sensitive to radiation. The photothermal efficiency of conventional LMs nanoparticles is about 7%, while the photothermal efficiency of Au-LM nanoparticles is about 22%. It can be used for photothermal and X-ray radiation therapy to treat cancer. Compared with Cu-LM, Au-LM nanoparticles have better stability and biocompatibility.[127]

Dealloying is one of the main methods for manufacturing nanoporous materials. In the past 10 years, researchers have discovered that the atomic interaction between the high-temperature liquid metallic melt and the alloy components leads to the separation of specific components from the alloy

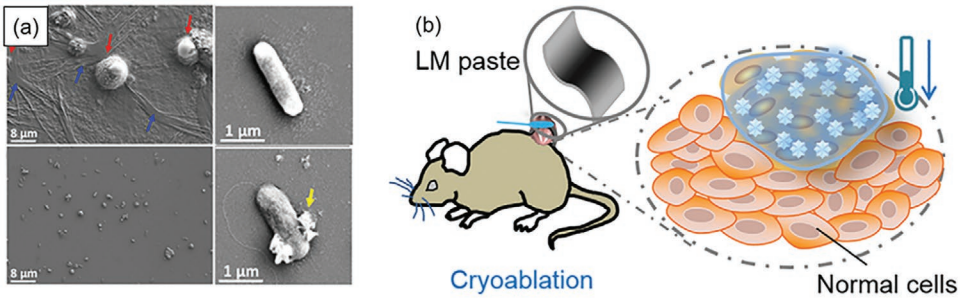

Figure 10. The applications of LMs and TMs combined in biomedical, a) Fe and LMs mixed to produce a Magnetic micromaterial to kill *P. aeruginosa* cells and *S. aureus* cells. Reproduced with permission.[39] Copyright 2020, ACS. b) Cu and LMs mixed to prepare plastic high thermal conductivity material used as a compress to treat cancer by cryotherapy to enhance thermal conductivity. Reproduced with permission.[43] Copyright 2020, ACS.

solids. It has been found that the liquid state of the metal is beneficial to the dealloying process, and the gallium-based LMs may support some new low-temperature dealloying methods. Zhang et al.[160] reported that Au, Ag, and Cu are dissolved in Ga to make alloys within 200 °C, cooled and solidified, and then Ga is etched away with acid and alkali solutions to prepare nanoporous structures. The temperature required by this method is much lower than the temperature required for the preparation of precursor alloys and dealloying processes in other methods. Select appropriate conditions for the reaction,[161] and use LMs dealloying technology to process micro-nano pores on the metal substrate may play a role in the field of microporous drug delivery.

5. Discussion and Outlook

LMs have a low melting point and better performance in terms of heat transfer and heat dissipation than most fluids. However, it will corrode many other types of metals and form alloy compounds. For this reason, studying its corrosion conditions and mechanisms is necessary, which is conducive to taking advantage of LMs as a flexible composite material with high thermal and electrical conductivity. Simultaneously, combining LMs and TMs can form alloy compounds. The physical and chemical properties of the new substances produced are different from those of the raw metals. The conditions for the formation of alloy compounds are studied, and the physical and chemical properties, lattice types and crystal characteristics of these alloy compounds are determined in this review. Mechanical properties such as toughness and Young's modulus can enrich the material library and provide data support for future scientific development and production. More researches on the characteristics of LMs and applications based on LMs will be discovered. After the combination of LMs and other metals, corrosion, internalization, infiltration, and other phenomena can be applied to manufacture new LM-based materials, improving the performance of LMs and broadening the application field of LM. At the same time, it is worth studying to explore the preparation nanomaterials with low energy consumption and phase transition theory at low temperature by using the unique characteristics of LMs.

The primary research goal in the future will be to reduce harmful corrosion of LMs and other metals. When using LMs as a liquid lubricant, it is necessary to consider that the LMs are oxidized by air under long-term working conditions, and it will corrode stainless steel at the same time, especially if it is used for a long time at high temperature, serious corrosion will occur on the surface in the research of scholars. In future research and industry, methods such as assembling such mechanical devices with coatings or alloys that are compatible with LMs may be used to solve this type of problem. Studies have shown that by adding metal elements such as Ti that are not easily soluble in Ga to metal base materials such as Fe, it is beneficial to slow down the corrosion of LMs and TMs. However, the added new elements will affect the physical and mechanical properties of the original metal, which is another problem that needs to be considered. The degree of corrosion is related to external conditions such as contact area, temperature, time, and other factors. It is also an effective anticorrosion strategy that intermetallic compounds can slow the penetration of elements. When the properties of the material itself cannot be changed, the contact area can be reduced and the contact between LMs and TM can be blocked by coating technology to control the contact temperature and time and other methods to reduce corrosion.

The second is to enhance the controllability of the combination of LMs and other materials. This is of great significance for the manufacture of LM-based metal composite products and the extension of their service life. When LMs and TMs are blended to prepare new materials, different environments such as oxygen-free environment, acid-base environment, and air endows LMs compounds different properties due to the particularity of the metal surface oxide layer. During the preparation process, if LMs are severely oxidized, the fluidity, electrical, and thermal conductivity will get worse, but the plasticity will be improved. Therefore, studying the conditions of the preparation process including reaction time, temperature, pH, oxygen concentration, and the ratio of materials before mixing, has an impact on the physical and chemical properties of the product, which is very meaningful for improving the material library and subsequent applications. Based on the combination of the different functional properties of various types of TM and the unique characteristics of LM, these products are expected to develop new applications in the fields of machinery, electromagnetics, biology, and microsystems.

The low melting point of LMs allows LMs to undergo phase change at lower temperatures, which provides achievable experimental conditions for the study of the underlying theories of metal phase change processes. At the same time, the oxidation layer of LMs affects the phase change process of LMs, and in the process of Bi-Ga solidification, complex patterns and abnormal phase enrichment appear on the surface. This surface coagulation effect can theoretically be applied to construct nanostructures of high melting point metals at low temperature.[162] The use of ultrasound, bubbles, electrical stimulation, and other ways to achieve LMs phase separation to prepare a new composite nanofunctional materials, has been widely studied. After adding MS to LMs in the form of solvents, polymorphic alloys and intermetallic compounds are formed and further processing is carried out, which will lead to more possibilities.[163]

With the extensive application research of liquid metal-based biomaterials in clinical, biosensing, implantable devices, the exploration of the comprehensive degradation mechanism of each use in vivo will promote its better development. The complex environment in the living body makes metal materials inevitably corroded, a series of electrochemical reactions may occur in the environment of body fluids, and some substances that are toxic to living bodies would be produced. Exploring the reaction mechanism and products of the combination of LMs and TMs in different environments is a prerequisite for ensuring that LMs and TMs work safely in the body. For metals that are not degradable in the body, developing strategies for metal recovery and enrichment is also an urgent problem need to be solved.

Acknowledgements

This work was supported by National Natural Science Foundation of China (Grant No. 81801794), Beijing Natural Science Foundation (Grant No. 7202104).

Conflict of Interest

The authors declare no conflict of interest.

Keywords

applications, chemical mechanisms, liquid metals, multifunctional materials, transition metals

Received: June 1, 2021
Revised: August 23, 2021
Published online: November 21, 2021

[1] M. D. Dickey, R. C. Chiechi, R. J. Larsen, E. A. Weiss, D. A. Weitz, G. M. Whitesides, *Adv. Funct. Mater.* **2008**, *18*, 1097.
[2] M. R. Khan, C. B. Eaker, E. F. Bowden, M. D. Dickey, **2014**, *111*, 14047.
[3] T. Liu, P. Sen, C. Kim, *J. Microelectromech. Syst.* **2012**, *21*, 443.
[4] Q. Wang, Y. Yu, J. Liu, **2018**, *20*, 1700781.
[5] M. J. Regan, H. Tostmann, P. S. Pershan, O. M. Magnussen, E. DiMasi, B. M. Ocko, M. Deutsch, *Phys. Rev. B* **1997**, *55*, 10786.
[6] K. B. Ozutemiz, J. Wissman, O. B. Ozdoganlar, C. Majidi, **2018**, *5*, 1701596.
[7] X. Zhao, S. Xu, J. Liu, *Front. Energy* **2017**, *11*, 535.
[8] S. Xu, B. Yuan, Y. Hou, T. Liu, J. Fu, J. Liu, *J. Phys. D: Appl. Phys.* **2019**, *52*, 353002.
[9] W. Zhang, B. S. Naidu, J. Z. Ou, A. P. O'Mullane, A. F. Chrimes, B. J. Carey, Y. Wang, S. Y. Tang, V. Sivan, A. Mitchell, S. K. Bhargava, K. Kalantar-Zadeh, *ACS Appl. Mater. Interfaces* **2015**, *7*, 1943.
[10] J. Zhang, Y. Yao, J. Liu, *Sci. Bull.* **2015**, *60*, 943.
[11] K.-Q. Ma, J. Liu, *Phys. Lett. A* **2007**, *361*, 252.
[12] S. Tan, Y. Zhou, L. Wang, J. Liu, *Sci. China: Technol. Sci.* **2016**, *59*, 301.
[13] X.-H. Yang, J. Liu, *Front. Energy* **2018**, *12*, 259.
[14] R. Guo, H. Wang, X. Sun, S. Yao, H. Chang, H. Wang, J. Liu, Y. Zhang, *ACS Appl. Mater. Interfaces* **2019**, *11*, 30019.
[15] C. Ladd, J. H. So, J. Muth, M. D. Dickey, *Adv. Mater.* **2013**, *25*, 5081.
[16] K. N. Paracha, A. D. Butt, A. S. Alghamdi, S. A. Babale, P. J. Soh, *Sensors* **2019**, *20*, 177.
[17] J. Wei, B. Wang, Z. Li, Z. Wu, M. Zhang, N. Sheng, Q. Liang, H. Wang, S. Chen, *Carbohydr. Polym.* **2020**, *238*, 116207.
[18] M. D. Dickey, *Adv. Mater.* **2017**, *29*, 1606425.
[19] G. Dong, S. Li, M. Yao, Z. Zhou, Y.-Q. Zhang, X. Han, Z. Luo, J. Yao, B. Peng, Z. Hu, H. Huang, T. Jia, J. Li, W. Ren, Z.-G. Ye, X. Ding, J. Sun, C.-W. Nan, L.-Q. Chen, J. Li, M. Liu, *Science* **2019**, *366*, 475.
[20] R. Guo, X. Wang, H. Chang, W. Yu, S. Liang, W. Rao, J. Liu, *Adv. Eng. Mater.* **2018**, *20*,1800054.
[21] A. Hirsch, S. P. Lacour, *Adv. Sci.* **2018**, *5*, 1800256.
[22] S. Handschuh-Wang, Y. Chen, L. Zhu, T. Gan, X. Zhou, *Langmuir* **2019**, *35*, 372.
[23] O. Oloye, C. Tang, A. Du, G. Will, A. P. O'Mullane, *Nanoscale* **2019**, *11*, 9705.
[24] R. David, N. Miki, *Nanoscale* **2019**, *11*, 21419.
[25] R. David, N. Miki, *Langmuir* **2018**, *34*, 10550.
[26] K. J. Kim, B. N. Harmon, L. Y. Chen, D. W. Lynch, *Phys. Rev. B* **1990**, *42*, 8813.
[27] S. Kulkarni, A. Pandey, S. Mutalik, *Nanomedicine* **2020**, *26*, 102175.
[28] Y. Cui, Y. Ding, S. Xu, Z. Yang, P. Zhang, W. Rao, J. Liu, *Int. J. Thermophys.* **2018**, *39*, 113.
[29] Y. Yu, E. Miyako, *iScience* **2018**, *3*, 134.
[30] P. Li, Y. Zhang, Z. Zheng, *Adv. Mater.* **2019**, *31*, 1902987.
[31] T. V. Neumann, M. D. Dickey, *Adv. Mater. Technol.* **2020**, *5*, 2000070.
[32] Y. Ren, X. Sun, J. Liu, *Micromachines* **2020**, *11*, 200.
[33] E. B. Secor, A. B. Cook, C. E. Tabor, M. C. Hersam, *Adv. Electron. Mater.* **2018**, *4*, 1700483.
[34] Y. Sun, S. Xu, S. Tan, J. Liu, *Micromachines* **2018**, *9*, 192.
[35] M.-g. Kim, H. Alrowais, S. Pavlidis, O. Brand, *Adv. Funct. Mater.* **2017**, *27*, 1604466.
[36] L. Tang, S. Cheng, L. Zhang, H. Mi, L. Mou, S. Yang, Z. Huang, X. Shi, X. Jiang, *iScience* **2018**, *4*, 302.
[37] Q. Wang, Y. Yu, J. Yang, J. Liu, *Adv. Mater.* **2015**, *27*, 7109.
[38] F. Li, J. Shu, L. Zhang, N. Yang, J. Xie, X. Li, L. Cheng, S. Kuang, S.-Y. Tang, S. Zhang, W. Li, L. Sun, D. Sun, *Appl. Mater. Today* **2020**, *19*, 100597.
[39] A. Elbourne, S. Cheeseman, P. Atkin, N. P. Truong, N. Syed, A. Zavabeti, M. Mohiuddin, D. Esrafilzadeh, D. Cozzolino, C. F. McConville, M. D. Dickey, R. J. Crawford, K. Kalantar-Zadeh, J. Chapman, T. Daeneke, V. K. Truong, *ACS Nano* **2020**, *14*, 802.
[40] L. Hu, H. Wang, X. Wang, X. Liu, J. Guo, J. Liu, *ACS Appl. Mater. Interfaces* **2019**, *11*, 8685.
[41] A. d. C. I, A. F. Chrimes, A. Zavabeti, K. J. Berean, B. J. Carey, J. Zhuang, Y. Du, S. X. Dou, K. Suzuki, R. A. Shanks, R. Nixon-Luke, G. Bryant, K. Khoshmanesh, K. Kalantar-Zadeh, T. Daeneke, *Nano Lett.* **2017**, *17*, 7831.
[42] J. Jeon, J. B. Lee, S. K. Chung, D. Kim, *Lab Chip* **2016**, *17*, 128.
[43] Y. Hou, P. Zhang, D. Wang, J. Liu, W. Rao, *ACS Appl. Mater. Interfaces* **2020**, *12*, 27984.
[44] W. E. Frazier, *J. Mater. Eng. Perform.* **2014**, *23*, 1917.
[45] L. Gardner, *Prog. Struct. Eng. Mater.* **2005**, *7*, 45.
[46] R. P. Tye, in *Thermal Conductivity*, Vol. *14* (Eds: P. G. Klemens, T. K. Chu), Springer US, Boston, MA **1976**, p. 217.
[47] J. Wadsworth, F. H. Froes, *JOM* **1989**, *41*, 12.
[48] J. Schreiber, V. Melov, presented at *Nondestructive Characterization of Materials XI*, Springer, Berlin **2003**, p. 833.
[49] F. Barbier, J. Blanc, *J. Mater. Res.* **2011**, *14*, 737.
[50] S. H. Shin, J. J. Kim, J. A. Jung, K. J. Choi, I. C. Bang, J. H. Kim, *J. Nucl. Mater.* **2012**, *422*, 92.
[51] Y. Cui, F. Liang, Z. Yang, S. Xu, X. Zhao, Y. Ding, Z. Lin, J. Liu, *ACS Appl. Mater. Interfaces* **2018**, *10*, 9203.
[52] J. Guo, J. Cheng, S. Wang, Y. Yu, S. Zhu, J. Yang, W. Liu, *Mater. Lett.* **2018**, *228*, 17.
[53] Z. Wang, Y. Wang, H. Gao, J. Niu, J. Zhang, Z. Peng, Z. Zhang, *Nanoscale Horiz.* **2018**, *3*, 408.
[54] Y. Li, S. Zhang, Q. Ding, D. Feng, B. Qin, L. Hu, *Mater. Lett.* **2018**, *215*, 140.
[55] S. Liu, S. McDonald, Q. Gu, S. Matsumura, D. Qu, K. Sweatman, T. Nishimura, K. Nogita, *J. Electron. Mater.* **2019**, *49*, 128.
[56] G. T. Paganoto, D. M. Santos, T. C. S. Evangelista, M. C. C. Guimaraes, M. Carneiro, J. Ribeiro, *Sci. World J.* **2017**, *2017*, 8786013.
[57] Y. Sohn, K. Chu, *Mater. Lett.* **2020**, *265*, 127223.
[58] P. A. Lopes, H. Paisana, A. T. De Almeida, C. Majidi, M. Tavakoli, *ACS Appl. Mater. Interfaces* **2018**, *10*, 38760.
[59] Y. Cui, F. Liang, S. Xu, Y. Ding, Z. Lin, J. Liu, *Colloids Surf. A* **2019**, *569*, 102.
[60] Alloy Phase Diagrams, *Bull. Alloy Phase Diagrams* **1985**, *6*, 566.

[61] S. Liu, D. Qu, S. McDonald, Q. Gu, S. Matsumura, K. Nogita, *J. Alloys Compd.* **2020**, *826*, 154221.
[62] S.-k. Lin, C.-l. Cho, H.-m. Chang, *J. Electron. Mater.* **2013**, *43*, 204.
[63] S. P. Yatsenko, N. A. Sabirzyanov, A. S. Yatsenko, *J. Phys.: Conf. Ser.* **2008**, *98*, 062032.
[64] S.-C. Lim, C.-Y. Chan, K.-T. Chen, H.-Y. Tuan, *Electrochim. Acta* **2019**, *297*, 288.
[65] M. Li, C. Li, F. Wang, W. Zhang, *Intermetallics* **2006**, *14*, 826.
[66] Y. Wang, Z. Wang, J. Zhang, C. Zhang, H. Gao, J. Niu, Z. Zhang, *Nanoscale* **2018**, *10*, 17070.
[67] M. M. Yazdanpanah, S. A. Harfenist, A. Safir, R. W. Cohn, *J. Appl. Phys.* **2005**, *98*, 073510.
[68] A. Hirsch, H. O. Michaud, A. P. Gerratt, S. de Mulatier, S. P. Lacour, *Adv. Mater.* **2016**, *28*, 4507.
[69] R. P. Elliott, F. A. Shunk, *Bull. Alloy Phase Diagrams* **1981**, *2*, 356.
[70] N. Eustathopoulos, R. Voytovych, *J. Mater. Sci.* **2015**, *51*, 425.
[71] X. Zhou, X. Li, K. Cheng, X. Huai, *J. Heat Transfer* **2018**, *140*, 081901.
[72] J. Zhang, R. Guo, J. Liu, *J. Mater. Chem. B* **2016**, *4*, 5349.
[73] P. A. Sørensen, S. Kiil, K. Dam-Johansen, C. E. Weinell, *J. Coat. Technol. Res.* **2009**, *6*, 135.
[74] W. Deqing, S. Ziyuan, Z. Longjiang, *Appl. Surf. Sci.* **2003**, *214*, 304.
[75] H. Wang, Y. Liu, *Friction* **2020**, *8*, 1007.
[76] O. Y. Fajardo, F. Bresme, A. A. Kornyshev, M. Urbakh, *J. Phys. Chem. Lett.* **2015**, *6*, 3998.
[77] J. Guo, J. Cheng, H. Tan, S. Zhu, Z. Qiao, J. Yang, W. Liu, *Materialia* **2018**, *4*, 10.
[78] H. Li, P. Tian, H. Lu, W. Jia, H. Du, X. Zhang, Q. Li, Y. Tian, *ACS Appl. Mater. Interfaces* **2017**, *9*, 5638.
[79] D. Kim, J.-B. Lee, *J. Korean Phys. Soc.* **2015**, *66*, 282.
[80] J. Jeon, J. B. Lee, S. K. Chung, D. Kim, presented at TRANSDUCERS 2015 –2015 18th International Solid-State Sensors, Actuators and Microsystems Conference, Anchorage, Alaska, June **2015**.
[81] J. Jeong, J. Seo, S. K. Chung, J.-B. Lee, D. Kim, *J. Microelectromech. Syst.* **2020**, *29*, 1208.
[82] A. W. Combs, W. A. Shiroma, Ohta, *Electron. Lett.* **2017**, *54*, 151.
[83] F. Carle, K. Bai, J. Casara, K. Vanderlick, E. Brown, *Phys. Rev. Fluids* **2017**, *2*, 013301.
[84] H. Wang, B. Yuan, S. Liang, R. Guo, W. Rao, X. Wang, H. Chang, Y. Ding, J. Liu, L. Wang, *Mater. Horiz.* **2018**, *5*, 222.
[85] R. Guo, X. Sun, B. Yuan, H. Wang, J. Liu, *Adv. Sci.* **2019**, *6*, 1901478.
[86] H. Wang, S. Chen, H. Li, X. Chen, J. Cheng, Y. Shao, C. Zhang, J. Zhang, L. Fan, H. Chang, R. Guo, X. Wang, N. Li, L. Hu, Y. Wei, J. Liu, *Adv. Funct. Mater.* **2021**, *31*, 2100274.
[87] X. Li, M. Li, L. Zong, X. Wu, J. You, P. Du, C. Li, *Adv. Funct. Mater.* **2018**, *28*, 1804197.
[88] S. Chen, Y. Ding, Q. Zhang, L. Wang, J. Liu, *Sci. China Mater.* **2018**, *62*, 407.
[89] M. Mohammed, R. Sundaresan, M. D. Dickey, *ACS Appl. Mater. Interfaces* **2015**, *7*, 23163.
[90] S. Liu, G. Zeng, W. Yang, S. McDonald, Q. Gu, S. Matsumura, K. Nogita, *ACS Appl. Mater. Interfaces* **2020**, *12*, 21045.
[91] J.-L. Ma, H.-X. Dong, Z.-Z. He, *Mater. Horiz.* **2018**, *5*, 675.
[92] B. Ma, C. Xu, J. Chi, J. Chen, C. Zhao, H. Liu, *Adv. Funct. Mater.* **2019**, *29*, 1901370.
[93] Y. Shi, M. Song, Y. Zhang, C. Zhang, H. Gao, J. Niu, W. Ma, J. Qin, Z. Zhang, *J. Power Sources* **2019**, *437*, 226889.
[94] O. I. Tikhomirova, M. V. Pikunov, L. P. Ruzinov, I. D. Marchukova, *Mater. Sci.* **1972**, *5*, 586.
[95] A. I. Ancharov, T. F. Grigoryeva, A. P. Barinova, V. V. Boldyrev, *Russ. Metall.* **2008**, *6*, 475.
[96] S. Ki, J. Shim, S. Oh, E. Koh, D. Seo, S. Ryu, J. Kim, Y. Nam, *Int. J. Heat Mass Transfer* **2021**, *170*, 121012.
[97] J. Shu, Y. Lu, E. Wang, X. Li, S. Y. Tang, S. Zhao, X. Zhou, L. Sun, W. Li, S. Zhang, *ACS Appl. Mater. Interfaces* **2020**, *12*, 11163.
[98] J. Tang, X. Zhao, J. Li, R. Guo, Y. Zhou, J. Liu, *ACS Appl. Mater. Interfaces* **2017**, *9*, 35977.
[99] J. Tang, X. Zhao, J. Li, Y. Zhou, J. Liu, *Adv. Sci.* **2017**, *4*, 1700024.
[100] A. F. Silva, H. Paisana, T. Fernandes, J. Góis, A. Serra, J. F. J. Coelho, A. T. de Almeida, C. Majidi, M. Tavakoli, *Adv. Mater. Technol.* **2020**, *5*, 2000343.
[101] T. Daeneke, K. Khoshmanesh, N. Mahmood, I. A. de Castro, D. Esrafilzadeh, S. J. Barrow, M. D. Dickey, K. Kalantar-Zadeh, *Chem. Soc. Rev.* **2018**, *47*, 4073.
[102] A. N. Campbell, W. F. Reynolds, *Can. J. Chem.* **1962**, *40*, 37.
[103] J. Mingear, D. Hartl, *Corros. Sci.* **2020**, *167*, 108524.
[104] M. Xiong, Y. Gao, J. Liu, *J. Magn. Magn. Mater.* **2014**, *354*, 279.
[105] S. Chen, X. Yang, Y. Cui, J. Liu, *ACS Appl. Mater. Interfaces* **2018**, *10*, 22889.
[106] H. Chang, R. Guo, Z. Sun, H. Wang, Y. Hou, Q. Wang, W. Rao, J. Liu, *Adv. Mater. Interfaces* **2018**, *5*, 1800571.
[107] S. Merhebi, M. Mayyas, R. Abbasi, M. J. Christoe, J. Han, J. Tang, M. A. Rahim, J. Yang, T. T. Tan, D. Chu, J. Zhang, S. Li, C. H. Wang, K. Kalantar-Zadeh, F. M. Allioux, *ACS Appl. Mater. Interfaces* **2020**, *12*, 20119.
[108] Y. Liu, J. Li, W. Zhang, *Chem. Commun.* **2020**, *56*, 6229.
[109] H. Okamoto, *ASM Alloy Phase Diagrams Center (Bismuth-Indium)*, Vol. *2*, **1990**.
[110] R. Johnson, *J. Phys. Rev. B* **1989**, *39*, 12554.
[111] R. C. Chiechi, E. A. Weiss, M. D. Dickey, G. M. Whitesides, *Angew. Chem.* **2008**, *120*, 148.
[112] O. Oloye, J. F. S. Fernando, E. R. Waclawik, D. Golberg, A. P. O'Mullane, *New J. Chem.* **2020**, *44*, 14979.
[113] S. Handschuh-Wang, Y. Chen, L. Zhu, X. Zhou, *ChemPhysChem* **2018**, *19*, 1584.
[114] R. K. Kramer, J. W. Boley, H. A. Stone, J. C. Weaver, R. J. Wood, *Langmuir* **2014**, *30*, 533.
[115] K. Doudrick, S. Liu, E. M. Mutunga, K. L. Klein, V. Damle, K. K. Varanasi, K. Rykaczewski, *Langmuir* **2014**, *30*, 6867.
[116] E. Saiz, A. P. Tomsia, *Nat. Mater.* **2014**, *3*, 903.
[117] S. Y. Tang, I. D. Joshipura, Y. Lin, K. Kalantar-Zadeh, A. Mitchell, K. Khoshmanesh, M. D. Dickey, *Adv. Mater.* **2016**, *28*, 604.
[118] W. Kong, Z. Wang, M. Wang, K. C. Manning, A. Uppal, M. D. Green, R. Y. Wang, K. Rykaczewski, *Adv. Mater.* **2019**, *31*, 1904309.
[119] J. Zhang, P. Hosemann, S. Maloy, *J. Nucl. Mater.* **2010**, *404*, 82.
[120] J. Zhang, N. Li, *J. Nucl. Mater.* **2008**, *373*, 351.
[121] O. A. Khudhair, R. A. Anaee, K. M. Shabeeb, *J. Bio- Tribo-Corros.* **2019**, *6*, 18.
[122] Z. Chao, A. O. Jian-Ping, W. Li, J. Tao, S. U. N. Guo-Zhong, H. E. Qing, Z. Zhi-Qiang, S. U. N. Yun, *Acta Phys. Chim. Sin.* **2012**, *28*, 1913.
[123] N. Haldolaarachchige, A. B. Karki, W. A. Phelan, Y. M. Xiong, R. Jin, J. Y. Chan, S. Stadler, D. P. Young, *J. Appl. Phys.* **2011**, *109*, 103712.
[124] C. S. Lue, W. J. Lai, Y. K. Kuo, *J. Alloys Compd.* **2005**, *392*, 72.
[125] A. E. Gunnæs, A. Olsen, P. T. Zagierski, O. B. Klewe, A. Aasen, *Z. Kristallogr.* **1998**, *213*, 639.
[126] Y. h. Wu, Z. f. Deng, Z. f. Peng, R. m. Zheng, S. q. Liu, S. t. Xing, J. y. Li, D. q. Huang, L. Liu, *Adv. Funct. Mater.* **2019**, *29*, 1903840.
[127] Z. Guo, J. Lu, D. Wang, W. Xie, Y. Chi, J. Xu, N. Takuya, J. Zhang, W. Xu, F. Gao, H. Wu, L. Zhao, *Bioact. Mater.* **2021**, *6*, 602.
[128] J. E. Norkett, M. D. Dickey, V. M. Miller, *Metall. Mater. Trans. A* **2021**, *52*, 2158.
[129] Y.-G. Deng, J. Liu, *Appl. Phys. A* **2009**, *95*, 907.
[130] F. Hoshyargar, J. Crawford, A. P. O'Mullane, *J. Am. Chem. Soc.* **2017**, *139*, 1464.
[131] V. B. Kumar, I. Perelshtein, G. Kimmel, Z. e. Porat, A. Gedanken, *J. Alloys Compd.* **2015**, *637*, 538.
[132] S. T. Liang, H. Z. Wang, J. Liu, *Chemistry* **2018**, *24*, 17616.
[133] A. Zavabeti, J. Z. Ou, B. J. Carey, N. Syed, R. Orrell-Trigg, E. L. H. Mayes, C. L. Xu, O. Kavehei, A. P. O'Mullane, R. B. Kaner, K. Kalantar-Zadeh, T. Daeneke, *Science* **2017**, *358*, 332.

[134] K. Arakawa, K. Yamamoto, K. Sakai, H. Koizumi, *Mater. Trans.* **2014**, *55*, 653.
[135] O. K. Chopra, D. L. Smith, P. F. Tortorelli, J. H. DeVan, D. K. Sze, *Fusion Technol.* **2017**, *8*, 1956.
[136] X. Wang, W. Yao, R. Guo, X. Yang, J. Tang, J. Zhang, W. Gao, V. Timchenko, J. Liu, *Adv. Healthcare Mater.* **2018**, *7*, 1800318.
[137] A. Gannarapu, B. A. Gozen, *Adv. Mater. Technol.* **2016**, *1*, 1600047.
[138] S. Guo, R. Lin, L. Wang, S. Lau, Q. Wang, R. Liu, *Mater. Sci. Eng. C* **2019**, *99*, 735.
[139] S. Kim, J. Oh, D. Jeong, J. Bae, *ACS Appl. Mater. Interfaces* **2019**, *11*, 20557.
[140] F. Studt, I. Sharafutdinov, F. Abild-Pedersen, C. F. Elkjaer, J. S. Hummelshoj, S. Dahl, I. Chorkendorff, J. K. Norskov, *Nat. Chem.* **2014**, *6*, 320.
[141] A. L. Lereu, F. Lemarchand, M. Zerrad, M. Yazdanpanah, A. Passian, *J. Appl. Phys.* **2015**, *117*, 063110.
[142] A. M. V. Mohan, N. H. Kim, Y. Gu, A. J. Bandodkar, J.-M. You, R. Kumar, J. F. Kurniawan, S. Xu, J. Wang, *Adv. Mater. Technol.* **2017**, *2*, 1600284.
[143] J. Wang, G. Cai, S. Li, D. Gao, J. Xiong, P. S. Lee, *Adv. Mater.* **2018**, *30*, 1706157.
[144] C. A. Silva, J. lv, L. Yin, I. Jeerapan, G. Innocenzi, F. Soto, Y. G. Ha, J. Wang, *Adv. Funct. Mater.* **2020**, *30*, 2002041.
[145] Y. Wang, S. Wang, H. Chang, W. Rao, *Adv. Mater. Interfaces* **2020**, *7*, 2000626.
[146] R. Zheng, Z. Peng, Y. Fu, Z. Deng, S. Liu, S. Xing, Y. Wu, J. Li, L. Liu, *Adv. Funct. Mater.* **2020**, *30*, 1910524.
[147] Y. G. Park, H. Kim, S. Y. Park, J. Y. Kim, J. U. Park, *ACS Appl. Mater. Interfaces* **2019**, *11*, 41497.
[148] M. Tavakoli, M. H. Malakooti, H. Paisana, Y. Ohm, D. G. Marques, P. A. Lopes, A. P. Piedade, A. T. de Almeida, C. Majidi, *Adv. Mater.* **2018**, *30*, 1801852.
[149] Y. Wang, W. Duan, C. Zhou, Q. Liu, J. Gu, H. Ye, M. Li, W. Wang, X. Ma, *Adv. Mater.* **2019**, *31*, 1905067.
[150] J. Guo, Y. Wang, X. Wang, Y. Xing, L. Hu, *Adv. Mater. Interfaces* **2020**, *7*, 2070117.
[151] J. Jeong, J. B. Lee, S. K. Chung, D. Kim, *Lab Chip* **2019**, *19*, 3261.
[152] F. Li, S. Kuang, X. Li, J. Shu, W. Li, S.-Y. Tang, S. Zhang, *Adv. Mater. Technol.* **2019**, *4*, 1800694.
[153] L. Cao, D. Yu, Z. Xia, H. Wan, C. Liu, T. Yin, Z. He, *Adv. Mater.* **2020**, *32*, 2000827.
[154] E. A. Redekop, V. V. Galvita, H. Poelman, V. Bliznuk, C. Detavernier, G. B. Marin, *ACS Catal.* **2014**, *4*, 1812.
[155] N. Taccardi, M. Grabau, J. Debuschewitz, M. Distaso, M. Brandl, R. Hock, F. Maier, C. Papp, J. Erhard, C. Neiss, W. Peukert, A. Gorling, H. P. Steinruck, P. Wasserscheid, *Nat. Chem.* **2017**, *9*, 862.
[156] M. Mayyas, M. Mousavi, M. B. Ghasemian, R. Abbasi, H. Li, M. J. Christoe, J. Han, Y. Wang, C. Zhang, M. A. Rahim, J. Tang, J. Yang, D. Esrafilzadeh, R. Jalili, F. M. Allioux, A. P. O'Mullane, K. Kalantar-Zadeh, *ACS Nano* **2020**, *14*, 14070.
[157] S. A. Idrus-Saidi, J. Tang, J. Yang, J. Han, T. Daeneke, A. P. O'Mullane, K. Kalantar-Zadeh, *ACS Sens.* **2020**, *5*, 1177.
[158] J. Li, X. Zhang, B. Yang, C. Zhang, T. Xu, L. Chen, L. Yang, X. Jin, B. Liu, *Chem. Mater.* **2021**, *33*, 4568.
[159] D. Wang, W. Xie, Q. Gao, H. Yan, J. Zhang, J. Lu, B. Liaw, Z. Guo, F. Gao, L. Yin, G. Zhang, L. Zhao, *Small* **2019**, *15*, 1900511.
[160] Z. Wang, H. Gao, J. Niu, C. Zhang, Z. Zhang, *ACS Sustainable Chem. Eng.* **2019**, *7*, 3274.
[161] J.-C. Shao, H.-J. Jin, *J. Mater. Sci.* **2020**, *55*, 8337.
[162] J. Tang, S. Lambie, N. Meftahi, A. J. Christofferson, J. Yang, M. B. Ghasemian, J. Han, F. M. Allioux, M. A. Rahim, M. Mayyas, T. Daeneke, C. F. McConville, K. G. Steenbergen, R. B. Kaner, S. P. Russo, N. Gaston, K. Kalantar-Zadeh, *Nat. Nanotechnol.* **2021**, *16*, 431.
[163] J. Tang, R. Daiyan, M. B. Ghasemian, S. A. Idrus-Saidi, A. Zavabeti, T. Daeneke, J. Yang, P. Koshy, S. Cheong, R. D. Tilley, R. B. Kaner, R. Amal, K. Kalantar-Zadeh, *Nat. Commun.* **2019**, *10*, 4645.

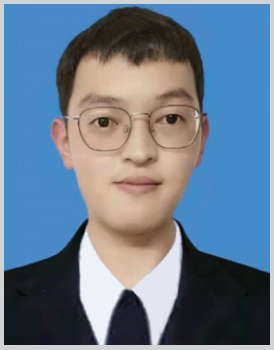

Yang Wang is a postgraduate student majoring in biomedical engineering at School of Biological Science and Medical Engineering, BUAA. His work focuses on physical and chemical properties and driving properties of liquid metals, applied in biomedicine.

Liang Hu is now an associate professor at Beijing Advanced Innovation Center for Biomedical Engineering, Beihang University. She received her bachelor and Ph.D. degrees at Zhejiang University. Her research ranges from the physiochemical of liquid metal interfacial properties to the 3D printing of liquid metal structures and functional devices.